



Defence Research and  
Development Canada

Recherche et développement  
pour la défense Canada



# **Unscented Kalman Filter Based Spatial- Temporal Registration Approach for Mobile Radar and ESM Sensors**

Yifeng Zhou, Winston Li and Henry Leung

**Defence R&D Canada – Ottawa**

TECHNICAL REPORT  
DRDC Ottawa TR 2003-219  
December 2003

Canada



# **Unscented Kalman Filter Based Spatial-Temporal Registration Approach for Mobile Radar and ESM Sensors**

Yifeng Zhou

Defence R&D Canada – Ottawa

Winston Li and Henry Leung

Department of Electrical and Computer Engineering, University of Calgary

**Defence R&D Canada – Ottawa**

Technical Report

DRDC Ottawa TR 2003-219

December 2003

© Her Majesty the Queen as represented by the Minister of National Defence, 2003

© Sa majesté la reine, représentée par le ministre de la Défense nationale, 2003

## **Abstract**

---

Space and time alignments are prerequisites for the successful fusion of multiple sensors. In this report, a space-time registration model is proposed for estimating the system biases and performing time synchronization for mobile radar and electronic support measure (ESM) systems. A space-time registration model for radar and ESM sensors is first developed, and an unscented Kalman filter (UKF) is proposed to estimate the space-time biases and target states simultaneously. The posterior Cramer-Rao bounds (PCRBs) are derived for the proposed UKF registration algorithm for ESM detection probability less than or equal to one. Theoretical analysis is performed for evaluating the accuracy and robustness of the proposed algorithm. Computer simulations are used to demonstrate the effectiveness and robustness of the proposed algorithm under different radar and ESM tracking scenarios.

## **Résumé**

---

Des alignements spatio-temporels sont requis pour faire la fusion de plusieurs capteurs. Dans ce rapport, un modèle d'alignement spatio-temporel est proposé dans le but d'estimer les biais du système et effectuer de la synchronisation en temps réel pour des systèmes de mesures de support électronique (ESM) radar mobiles. D'abord, un modèle d'alignement spatio-temporel pour des capteurs radar et ESM est développé, et un filtre de Kalman sans biais (Unscented Kalman Filter, UKF) est proposé pour estimer les biais spatio-temporels et les états des cibles simultanément. Les limites postérieures de Cramer-Rao (PCRB) sont dérivées pour l'algorithme d'alignement UKF proposé, pour une probabilité de détection ESM plus petite ou égale à l'unité. Une analyse théorique est effectuée pour évaluer la précision et la robustesse de l'algorithme proposé. On démontre l'efficacité et la robustesse de l'algorithme par simulations, avec plusieurs scénarios de poursuite radar et ESM.

This page intentionally left blank.

## Executive summary

---

The interest in fusing data from active radar and passive electronic support measures (ESM) has grown in recent years. The attribute information obtained by an ESM sensor can be combined with radar tracks through track association. The fusion of information by ESM and radar systems can be used to increase the likelihood of target acquisition and reduce vulnerability to jamming. It helps to improve situation awareness and provide more accurate and complete composite target track files. However, to fuse data successfully, radar and ESM sensors must be aligned, or registered, properly in both spatial and temporal domains. If the sensors are not registered adequately, it would introduce ghost tracks in the system coordinates and adversely affect the performance of fusion. It was found that if sensor registration errors are large, the fusion performance could be even worse than that of a single sensor application.

Registration of mobile radar and ESM sensors is an important problem encountered in air-launched and ship launched vehicle applications. However, although many sensor registration algorithms have been developed in the literature, they are all based on registration models that assume a perfect time alignment. In real applications, the time misalignment effect has to be considered in the registration process. In this report, a space-time registration model is proposed for estimating both the spatial system biases and the time synchronization offset for mobile radar and ESM sensors. A space-time registration model for radar and ESM sensors is developed and the unscented Kalman filter (UKF) is applied to estimate the space-time biases and target states simultaneously. Theoretical analysis is carried out which includes the posterior Cramer-Rao bound (PCRB), the effect of spatial-temporal biases upon target state estimation and the sensitivity of the UKF as well. We show that the target state estimates are unbiased if the space-time system biases are completely corrected. Computer simulations show that the UKF estimates of the registration parameters and target states are all close to their corresponding PCRBs under different track scenarios and detection probabilities for the ESM system. In the simulation studies, the UKF has demonstrated its superior stability to the extended Kalman filter (EKF).

Yifeng Zhou, Winston Li , Henry Leung. 2003. Unscented Kalman Filter Based Spatial-Temporal Registration Approach for Mobile Radar and ESM Sensors. DRDC Ottawa TR 2003-219. Defence R&D Canada - Ottawa.





## Sommaire

---

L'intérêt de la fusion de données en provenance de radars actifs et de systèmes de mesures de support électronique (ESM) passifs a augmenté au cours des quelques dernières années. Les informations d'attributs obtenues par un capteur ESM peuvent être combinées avec des pistes radar en faisant une association de piste. La fusion de l'information en provenance de systèmes ESM peuvent être combinées avec des pistes radar en faisant des associations de pistes. La fusion de l'information en provenance de systèmes ESM et radar peut être utilisée pour augmenter la probabilité d'acquisition de cible et réduire la vulnérabilité au brouillage. Elle aide à améliorer la connaissance de la situation ainsi que la précision et la complétude de fichiers de piste pour des cibles composites. Par contre, pour faire une fusion avec succès, il faut que les capteurs radar et ESM soient alignés dans le temps comme dans l'espace. Si les capteurs ne sont pas correctement alignés, cela introduit des pistes fantômes dans les coordonnées du système et affecte de façon adverse les performances de la fusion. Il a été observé que si les erreurs d'alignement des capteurs sont grandes, les performances de la fusion peuvent même être pires que celles d'une application monocapteur.

L'alignement de capteurs radar mobiles et de capteurs ESM est un problème important, rencontré dans des applications sur des véhicules aéroportés ainsi que maritimes. Par contre, bien que la littérature fait état de plusieurs algorithmes d'alignement, ceux-ci utilisent tous l'hypothèse que les capteurs sont parfaitement alignés dans le temps. En réalité, les effets des erreurs d'alignement temporel doivent être considérés dans le processus d'alignement. Dans ce rapport, un modèle d'alignement spatio-temporel est proposé pour estimer non seulement les biais du système d'alignement spatial, mais encore les décalages de synchronisation temporelle pour des radars et capteurs ESM mobiles. Un modèle d'alignement spatio-temporel pour radars et ESM est développé et le filtre Kalman sans biais (Unscented Kalman Filter, UKF) est appliqué pour estimer simultanément les biais spatio-temporels et les états des cibles. Une analyse théorique est faite, incluant la limite postérieure de Cramer-Rao (PCRB), l'effet de biais spatio-temporel sur l'estimation des états de cibles, ainsi que la sensibilité de UKF. Nous montrons que les estimés des états des cibles sont sans biais si les biais spatio-temporels du système sont totalement corrigés. Des simulations montrent que les estimés du UKF pour les paramètres d'alignement et des états des cibles sont tous proches de leur PCRB

pour différents scénarios de poursuite et différentes probabilités de détection pour des systèmes ESM. Dans les études de simulation, le UKF a montré une meilleure stabilité que le filtre de Kalman étendu.

Yifeng Zhou, Winston Li , Henry Leung. 2003. Unscented Kalman Filter Based Spatial-Temporal Registration Approach for Mobile Radar and ESM Sensors. DRDC Ottawa TR 2003-219. R&D pour la defense Canada - Ottawa.

# Table of contents

---

Abstract.....	i
Executive summary .....	iii
Sommaire.....	v
Table of contents .....	vii
List of figures .....	viii
1. Introduction .....	1
2. Space-Time Registration Model of Mobile Radar and ESM Sensors .....	3
3. UKF Based Space-Time Registration Method .....	7
4. Performance Analysis.....	11
4.1 Derivation of the PCRB.....	11
4.2 Effects of sensor biases on target state estimates .....	13
4.3 Sensitivity Analysis.....	15
5. Experimental Results.....	18
5.1 Constant-velocity targets .....	18
4.2 Constant-acceleration targets.....	25
6. Conclusions .....	29
7. References .....	30
Annex A.....	33
Annex B.....	34

## List of figures

---

Figure 1. Geometry of the space-time system biases for the mobile radar and ESM sensors. ...	6
Figure 2. Track plots of the constant-velocity targets. (a) actual tracks and the radar measurements; (b) actual and the fused tracks. ....	18
Figure 3. Variation of the MSEs of the registration error estimates versus the number of measurements for the constant-velocity target and a unity detection probability for the ESM sensor: (a) $\Delta t$ ; (b) $\Delta\theta_R$ ; (c) $\Delta r_R$ ; (d) $\Delta\theta_E$ .....	20
Figure 4. Variation of the MSEs of the target state estimates versus the number of measurements for the constant-velocity state and a unity detection probability for the ESM sensor: (a) position along x-axis; (b) position along y-axis; (c) velocity along x-axis; (d) velocity along y-axis. ....	21
Figure 5. Variation of the MSEs of the registration estimates versus the number of measurements for the constant-velocity target and a 75% detection probability for the ESM sensor: (a) $\Delta t$ ; (b) $\Delta\theta_R$ ; (c) $\Delta r_R$ ; (d) $\Delta\theta_E$ .....	22
Figure 6. Variation of the MSEs of the target state estimates versus the number of measurements for the constant-velocity target and a 75% detection probability for the ESM sensor: (a) position along x-axis; (b) position along y-axis; (c) velocity along x-axis; (d) velocity along y-axis. ....	23
Figure 7. Comparison of the state estimates with and without measuring the ESM sensor states: (a) the target position along x-axis; (b) the target position along y-axis; (c) the ESM position along x-axis; (d) the ESM position along y-axis. ....	24
Figure 8. Comparison of the EKF and UKF registration algorithms: (a) divergent EKF solution for radar range bias estimation; (b) convergent EKF for radar range bias estimation. ....	25
Figure 9. Track plots of the constant-acceleration targets. (a) actual tracks and the radar measurements; (b) actual and fused tracks. ....	25
Figure 10. Variation of the MSEs of the registration estimates versus the number of measurements for the constant-acceleration target and a unity detection probability for the ESM sensor: (a) $\Delta t$ ; (b) $\Delta\theta_R$ ; (c) $\Delta r_R$ ; (d) $\Delta\theta_E$ .....	27
Figure 11. Variation of the MSEs of the target state estimates versus the number of measurements for the constant-acceleration target and a unity detection probability for the ESM sensor: (a) position in x-axis; (b) position in y-axis; (c) velocity in x-axis; (d) velocity in y-axis; (e) acceleration in x-axis; (f) acceleration in y-axis. ....	28

# 1. Introduction

---

The interest in fusing data from multiple active and/or passive sensors has grown in recent years [1]-[3]. Data fusion can improve the accuracy of a surveillance system. Radar is a typical active sensor that provides both range and angle measurements, while the electronic support measure (ESM) system is an important passive sensor for detecting emitters. Features provided by an ESM include angle, time of arrival, frequency, and pulse width, etc [4]. The attribute information obtained by an ESM sensor can be combined with radar tracks through track association. The use of ESM and radar systems increases the likelihood of target acquisition and reduces vulnerability to jamming [5]-[7]. It helps to improve situation awareness and more accurate and complete composite target track files.

Registration refers to the process of ensuring the requisite error free coordinate conversion of multiple sensor data. It occurs in data fusion when the sensors are not aligned properly. Major source of registration errors can be classified into spatial and temporal errors. The spatial registration errors include the azimuth bias error with respect to a common reference and the range offset errors of each sensor. The temporal registration errors include timing errors, i.e., the clocks of each sensor may not be calibrated or synchronized. They may have time offset between one another. The inherent spatial system biases of a radar system include angle bias with respect to a common reference and the range offset errors, while ESM sensors are mainly affected by angle bias because they do not often measure the range of emitters. Registration errors are system errors and their effect is to introduce biases into fusion and therefore, to generate ghost targets for multisensor signal processing. To fuse data from different sensors successfully, sensors must be aligned properly in both spatial and temporal domains [8]-[10]. Registration can be considered as a two-phase process: sensor initialization and relative alignment. Sensor initialization registers each sensor independently with respect to the system coordinates. Once the sensor initialization is completed, we can start the relative sensor alignment procedure using common targets. In relative sensor alignment, a sufficient number of data points are collected to compute the system biases which are used to adjust subsequent incoming sensor data for further processing.

Many registration techniques have been developed in the literature for radar systems. These include the off-line methods such as the least-squares (LS) method [11]-[13], the maximum likelihood (ML) approach [14]-[15], and on-line approaches such as the Kalman filtering based approaches [16]-[19]. However, all these methods are developed based on a registration model that assumes that all the measurements from different sensors are perfectly aligned in time. In practice, the time misalignment

effect has to be considered in the registration process. Registration of mobile sensors is another important problem encountered in both air-launched and ship-launched vehicle applications [17][20]. In this report, a space-time registration method is proposed to jointly estimate the spatial and temporal biases of mobile radar and ESM sensors. A space-time registration model is first proposed. A combined state space model with these biases is then developed. An unscented Kalman filter (UKF) is applied to estimate the parameters for system biases, time misalignment, and target states simultaneously. The UKF is a relatively new nonlinear filtering algorithm [21]-[23] and has a better stability performance when compared to the most widely used extended Kalman filter (EKF) [22] in which the linearization and explicit calculations of Jacobian and Hessian matrix have often caused divergence. The posterior Cramer-Rao bound (PCRB) [26]-[27] is employed for assessing the performance of a registration algorithm. The PCRB is derived for random parameter estimation in a stochastic system while the regular CRB is a lower bound for the estimation of deterministic parameters. Since in the proposed registration model, the target states are random, the regular CRB is no longer an appropriate performance measure, we use the PCRB for the UKF registration estimates for ESM sensors of detection probability equal to or less than one, respectively. Theoretical performance and sensitivity analysis for the estimation bias is also carried out to evaluate the accuracy and robustness of the proposed UKF registration algorithm. The report is organized as follows. In Section 2, we introduce the space-time registration model for mobile radar and ESM sensors. The UKF registration algorithm is described in Section 3. The theoretical performance analyses are given in Section 4 including the PCRB derivation, the influence of the misalignment on the radar/ESM system and sensitivity analysis. In Section 5, we evaluate the performance of the UKF registration algorithm using computer-simulated data. Finally, the conclusions are given in Section 6.

## 2. Space-Time Registration Model of Mobile Radar and ESM Sensors

---

To register mobile radar and ESM sensors, a space-time system bias model and the corresponding state space representation must first be developed. Without loss of generality, two mobile sensors are considered here. Assume that A is a radar, and B is an ESM sensor as shown in Figure 1. Furthermore, assume that the radar is located at the origin of the common Cartesian coordinate system. Let  $\{u(t_k), v(t_k)\}$  denote the Cartesian coordinate of the ESM sensor relative to the radar at  $t_k$ , where  $t_k$  is the ESM sensor sampling time. Let  $\hat{t}_k$  for  $k=1, 2, \dots, K$  denote the radar sampling time, and  $\Delta t$  represent the difference in sampling times between the radar and the ESM sensor. The sampling time biases of these two sensors are then related by

$$\hat{t}_k = t_k + \Delta t, \quad k=1, 2, \dots, K. \quad (1)$$

Suppose that  $\{x_R(\hat{t}_k), y_R(\hat{t}_k)\}$  and  $\{\tilde{x}_R(\hat{t}_k), \tilde{y}_R(\hat{t}_k)\}$  are the state and measurement of the target according to the radar at time  $\hat{t}_k$ , and their corresponding polar coordinates are  $\{r_R(\hat{t}_k), \theta_R(\hat{t}_k)\}$  and  $\{\tilde{r}_R(\hat{t}_k), \tilde{\theta}_R(\hat{t}_k)\}$ , respectively. Let  $\{\Delta r_R, \Delta \theta_R\}$  denote the system bias of the radar in the range and angle, and  $\{\tilde{\theta}_E(t_k), \Delta \theta_E\}$  represents the angle measurement and system bias of the ESM sensor in the polar coordinate system. Let  $\{\hat{r}_R(\hat{t}_k), \hat{\theta}_R(\hat{t}_k)\}$  denote the radar measurement in the presence of system biases

$$\begin{aligned} \hat{r}_R(\hat{t}_k) &= r_R(\hat{t}_k) + \Delta r_R, \\ \hat{\theta}_R(\hat{t}_k) &= \theta_R(\hat{t}_k) + \Delta \theta_R. \end{aligned} \quad (2)$$

The measurement of the ESM sensor perturbed by the system biases is given by

$$\hat{\theta}_E(t_k) = \theta_E(t_k) + \Delta \theta_E. \quad (3)$$

The radar measurements can then be expressed as

$$\begin{aligned} \tilde{x}_R(\hat{t}_k) &= \hat{r}_R(\hat{t}_k) \sin[\hat{\theta}_R(\hat{t}_k)] + n_1(\hat{t}_k) \\ &= [r_R(t_k + \Delta t) + \Delta r_R] \sin[\theta_R(t_k + \Delta t) + \Delta \theta_R] + n_1(t_k + \Delta t), \\ \tilde{y}_R(\hat{t}_k) &= \hat{r}_R(\hat{t}_k) \cos[\hat{\theta}_R(\hat{t}_k)] + n_2(\hat{t}_k) \\ &= [r_R(t_k + \Delta t) + \Delta r_R] \cos[\theta_R(t_k + \Delta t) + \Delta \theta_R] + n_2(t_k + \Delta t) \end{aligned} \quad (4)$$

where  $n_i(t_k + \Delta t)$  is a zero mean white Gaussian noise process with variance  $\sigma_1^2$  for  $i=1, 2$ .

The polar and Cartesian coordinates of the target states are related by

$$\begin{aligned} r_R(t_k + \Delta t) &= \sqrt{x_R^2(t_k + \Delta t) + y_R^2(t_k + \Delta t)}, \\ \sin[\theta_R(t_k + \Delta t)] &= x_R(t_k + \Delta t)/r_R(t_k + \Delta t), \\ \cos[\theta_R(t_k + \Delta t)] &= y_R(t_k + \Delta t)/r_R(t_k + \Delta t). \end{aligned} \quad (5)$$

Assume that the system biases (including the time alignment error) are sufficiently small. Using a first-order approximation, (5) and (4) can be written as

$$\begin{aligned} \tilde{x}_R(t_k + \Delta t) &= x_R(t_k + \Delta t) + y_R(t_k + \Delta t)\Delta\theta_R + \sin[\theta_R(t_k + \Delta t)]\Delta r_R + n_1(t_k + \Delta t), \\ \tilde{y}_R(t_k + \Delta t) &= y_R(t_k + \Delta t) - x_R(t_k + \Delta t)\Delta\theta_R + \cos[\theta_R(t_k + \Delta t)]\Delta r_R + n_2(t_k + \Delta t), \end{aligned} \quad (6)$$

where higher order terms of the system biases are ignored. Consider the constant velocity model for the target and denote the state vector by  $\xi(t_k) = [x_R(t_k), \dot{x}_R(t_k), y_R(t_k), \dot{y}_R(t_k)]^T$ , where  $\{x_R(t_k), y_R(t_k)\}$  and  $\{\dot{x}_R(t_k), \dot{y}_R(t_k)\}$  are the position and speed of the target at time  $t_k$ . Let  $T$  denote the sensor sampling interval. The state equation of the target with respect to the radar can be expressed as

$$\xi(t_{k+1}) = \Phi \xi(t_k) + \Gamma \mu(t_k), \quad (7)$$

where  $\Phi = \begin{bmatrix} 1 & T & 0 & 0 \\ 0 & 1 & 0 & 0 \\ 0 & 0 & 1 & T \\ 0 & 0 & 0 & 1 \end{bmatrix}$ ,  $\Gamma = [T^2/2, T, T^2/2, T]^T$ , and  $\mu(t_k)$  is a white Gaussian noise process with

zero mean and variance  $\sigma_2^2$ .

The target position in the radar coordinate system at time  $\hat{t}_k = t_k + \Delta t$  can be derived from (7) as

$$\begin{aligned} x_R(t_k + \Delta t) &= x_R(t_k) + \dot{x}_R(t_k)\Delta t + \frac{\Delta t^2}{2} \mu(t_k), \\ y_R(t_k + \Delta t) &= y_R(t_k) + \dot{y}_R(t_k)\Delta t + \frac{\Delta t^2}{2} \mu(t_k). \end{aligned} \quad (8)$$

Substituting (8) into (6) and using a first-order approximation, the radar measurement model can be written as

$$\begin{aligned} \tilde{x}_R(t_k + \Delta t) &= x_R(t_k) + \dot{x}_R(t_k)\Delta t + y_R(t_k)\Delta\theta_R + \frac{x_R(t_k)}{\sqrt{x_R^2(t_k) + y_R^2(t_k)}} \Delta r_R + n_1(t_k + \Delta t), \\ \tilde{y}_R(t_k + \Delta t) &= y_R(t_k) + \dot{y}_R(t_k)\Delta t - x_R(t_k)\Delta\theta_R + \frac{y_R(t_k)}{\sqrt{x_R^2(t_k) + y_R^2(t_k)}} \Delta r_R + n_2(t_k + \Delta t). \end{aligned} \quad (9)$$

The same measurement equation for the constant-acceleration model can be obtained in a similar fashion.



Now we consider the measurement model for the ESM sensor,

$$\tilde{\theta}_E(t_k) = \hat{\theta}_E(t_k) + n_3(t_k) = \theta_E(t_k) + \Delta\theta_E + n_3(t_k), \quad (10)$$

where  $n_3(t_k)$  is a white Gaussian noise process with zero mean and variance  $\sigma_3^2$ . The true target states in the local coordinate of the ESM and radar sensor should be the same, and hence we have

$$\begin{aligned} x_R(t_k) &= r_R(t_k) \sin \theta_R(t_k) = r_E(t_k) \sin \theta_E(t_k) + u(t_k) \\ y_R(t_k) &= r_R(t_k) \cos \theta_R(t_k) = r_E(t_k) \cos \theta_E(t_k) + v(t_k), \end{aligned} \quad (11)$$

respectively. From (11) we have

$$\theta_E(t_k) = \text{artg} \left[ \frac{x_R(t_k) - u(t_k)}{y_R(t_k) - v(t_k)} \right], \quad (12)$$

and the ESM sensor measurement model becomes

$$\tilde{\theta}_E(t_k) = \text{artg} \left[ \frac{x_R(t_k) - u(t_k)}{y_R(t_k) - v(t_k)} \right] + \Delta\theta_E + n_3(t_k). \quad (13)$$

In the formulation, the dynamic model of the ESM sensor is derived with respect to the radar. Let  $\boldsymbol{\psi}(t_k) = [u(t_k), \dot{u}(t_k), v(t_k), \dot{v}(t_k)]^T$  denote the state vector of the ESM sensor, where  $\{\dot{u}(t_k), \dot{v}(t_k)\}$  is the relative speed of the ESM sensor with respect to the radar. The dynamic equation of the ESM sensor with respect to the radar is then given by

$$\boldsymbol{\psi}(t_{k+1}) = \boldsymbol{\Phi}\boldsymbol{\psi}(t_k) + \boldsymbol{\Gamma}\nu(t_k), \quad (14)$$

where  $\nu(t_k)$  is again assumed to be a white Gaussian noise process with zero mean and variance  $\sigma_\nu^2$ .

The radar measures the states of the ESM sensor to determine the relative motion between the two sensors. The space-time system biases  $\{\Delta t, \Delta\theta_R, \Delta r_R\}$  also exist in the ESM sensor state measurements by the radar. Let  $\{\tilde{u}(t_k + \Delta t), \tilde{v}(t_k + \Delta t)\}$  denote the ESM sensor states measured by the radar. Based on a first-order approximation, the radar measurement equation for the ESM sensor states can be derived as

$$\begin{aligned} \tilde{u}(t_k + \Delta t) &= u(t_k) + \dot{u}(t_k)\Delta t + v(t_k)\Delta\theta_R + \frac{u(t_k)}{\sqrt{u^2(t_k) + v^2(t_k)}} \Delta r_R + n_4(t_k + \Delta t) \\ \tilde{v}(t_k + \Delta t) &= v(t_k) + \dot{v}(t_k)\Delta t - u(t_k)\Delta\theta_R + \frac{v(t_k)}{\sqrt{u^2(t_k) + v^2(t_k)}} \Delta r_R + n_5(t_k + \Delta t). \end{aligned} \quad (15)$$

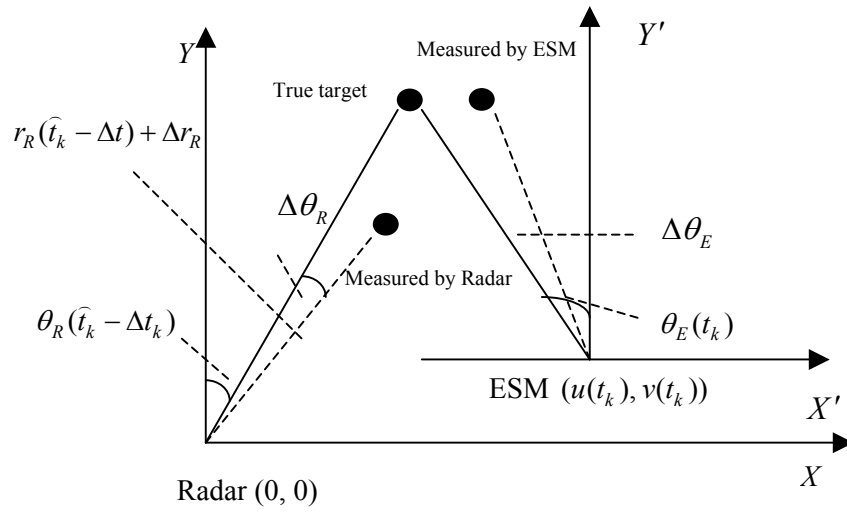


**Figure 1. Geometry of the space-time system biases for the mobile radar and ESM sensors.**

### 3. UKF Based Space-Time Registration Method

Using the state space models developed in the previous section, we proposed to solve the mobile radar/ESM registration problem by applying the Kalman filters. The UKF [22][28] is employed because of its robustness. The results will be compared with those of the EKF to demonstrate the stability advantage of the UKF.

The augmented state vector  $\mathbf{X}(t_k)$  is defined as  $\mathbf{X}(t_k)=[(\mathbf{X}^{(1)}(t_k))^T, (\mathbf{X}^{(2)}(t_k))^T]^T$ , where  $\mathbf{X}^{(1)}(t_k)=[\xi^T(t_k), \psi^T(t_k)]^T$ ,  $\xi(t_k)=[x_R(t_k), \dot{x}_R(t_k), y_R(t_k), \dot{y}_R(t_k)]^T$  is the target state vector in the local coordinate of the radar,  $\psi(t_k)=[u(t_k), \dot{u}(t_k), v(t_k), \dot{v}(t_k)]^T$  is the ESM sensor state vector, and  $\mathbf{X}^{(2)}(t_k)=[\Delta t, \Delta\theta_R, \Delta r_R, \Delta\theta_E]^T$  is the space-time system bias vector. The dynamic equation for the augmented state can be written as

$$\mathbf{X}(t_{k+1}) = \mathbf{F}\mathbf{X}(t_k) + \mathbf{n}_X(t_k), \quad (16)$$

where  $\mathbf{n}_X(t_k)=[\mathbf{I}\mu(t_k), \mathbf{I}\nu(t_k), \mathbf{0}]^T$ ,  $\mathbf{F} = \begin{bmatrix} \Phi & \mathbf{0} & \mathbf{0} \\ \mathbf{0} & \Phi & \mathbf{0} \\ \mathbf{0} & \mathbf{0} & \mathbf{I} \end{bmatrix}$ , and  $\mathbf{I}$  denotes the identity matrix.

Let  $\mathbf{Z}(t_k)=[\tilde{x}_R(t_k + \Delta t), \tilde{y}_R(t_k + \Delta t), \tilde{\theta}_E(t_k), \tilde{u}(t_k + \Delta t), \tilde{v}(t_k + \Delta t)]^T$  denote the augmented measurement vector and  $\mathbf{n}_z(t_k)=[n_1(t_k + \Delta t), n_2(t_k + \Delta t), n_3(t_k), n_4(t_k + \Delta t), n_5(t_k + \Delta t)]^T$  be the measurement noise vector. The augmented measurement equation can be expressed as

$$\mathbf{Z}(t_k) = \mathbf{h}(t_k) + \mathbf{n}_z(t_k), \quad (17)$$

where

$$\begin{aligned} \mathbf{h}(t_k) &= [h_1(t_k), h_2(t_k), h_3(t_k), h_4(t_k), h_5(t_k)]^T \\ h_1(t_k) &= x_R(t_k) + \dot{x}_R(t_k)\Delta t + y_R(t_k)\Delta\theta_R + \frac{x_R(t_k)}{\sqrt{x_R^2(t_k) + y_R^2(t_k)}}\Delta r_R \\ h_2(t_k) &= y_R(t_k) + \dot{y}_R(t_k)\Delta t - x_R(t_k)\Delta\theta_R + \frac{y_R(t_k)}{\sqrt{x_R^2(t_k) + y_R^2(t_k)}}\Delta r_R \\ h_3(t_k) &= \text{artg}\left[\frac{x_R(t_k) - u(t_k)}{y_R(t_k) - v(t_k)}\right] + \Delta\theta_E \end{aligned}$$

$$\begin{aligned}
h_4(t_k) &= u(t_k) + \dot{u}(t_k)\Delta t + v(t_k)\Delta\theta_R + \frac{u(t_k)}{\sqrt{u^2(t_k) + v^2(t_k)}} \Delta r_R \\
h_5(t_k) &= v(t_k) + \dot{v}(t_k)\Delta t - u(t_k)\Delta\theta_R + \frac{v(t_k)}{\sqrt{u^2(t_k) + v^2(t_k)}} \Delta r_R.
\end{aligned} \tag{18}$$

In practical situations, the ESM sensor measurements depend on the emission and scanning pattern of the emitters. They may not be available at certain sampling times. A detection sequence is used to address this miss detection problem. Let the detection sequence be defined as  $\mathbf{S}_l(t_K) = \{s_l(t_1), s_l(t_2), \dots, s_l(t_K)\}$ ,  $l = 1, 2, \dots, 2^K$ , where  $s_l(t_k) = 1$  when the target is detected, and  $s_l(t_k) = 0$  when the ESM sensor misses the target. The ESM measurement equation in (18) can be written as

$$h_3(t_k) = s_l(t_k) \left\{ \text{artg} \left[ \frac{x_R(t_k) - u(t_k)}{y_R(t_k) - v(t_k)} \right] + \Delta\theta_E \right\}. \tag{19}$$

Equations (16) and (17) form the state space and measurement models for the mobile radar/ESM registration problem. In the following, we apply the UKF to the models mentioned above for registration. The EKF formulation is given in Annex A. The UKF uses the unscented transformation (UT) [22] to estimate the mean and covariance of the augmented state and measurement. In the UT, the state distribution is computed by a set of special sample points called sigma points. Suppose that the dimension of the augmented state is  $L$ , then, the UT requires  $2L+1$  sigma points. The mean and covariance are approximated by a weighted sample mean and covariance of these sigma points. More precisely, given the augmented state estimate  $\hat{\mathbf{X}}(t_{k-1})$  and state covariance estimate  $\mathbf{P}(t_{k-1})$ , the sigma points are formed by

$$\begin{aligned}
\chi_0(t_{k-1}) &= \hat{\mathbf{X}}(t_{k-1}), \\
\chi_i(t_{k-1}) &= \hat{\mathbf{X}}(t_{k-1}) + \left( \sqrt{(L + \lambda)\mathbf{P}(t_{k-1})} \right)_i, \quad i = 1, 2, \dots, L, \\
\chi_i(t_{k-1}) &= \hat{\mathbf{X}}(t_{k-1}) - \left( \sqrt{(L + \lambda)\mathbf{P}(t_{k-1})} \right)_i, \quad i = L + 1, L + 2, \dots, 2L
\end{aligned} \tag{20}$$

where  $\lambda = \alpha^2(L + \kappa) - L$  is a scaling parameter,  $\alpha$ ,  $\beta$ , and  $\kappa$  are constants. The parameter  $\alpha$  determines the spread of the sigma points around  $\hat{\mathbf{X}}(t_{k-1})$  and is usually set to a small positive value.  $\kappa$  is a secondary scaling parameter while  $\beta$  is a parameter depending on the distribution of the estimates. For Gaussian distributions,  $\beta = 2$  is optimal.  $\left( \sqrt{(L + \lambda)\mathbf{P}(t_{k-1})} \right)_i$  is the  $i$ th column of the matrix square

root. The matrix square root  $V$  of the state covariance matrix  $P$  is defined as  $VV^T = P$ . These sigma points can be updated using the state equation,

$$\chi_i(t_k | t_{k-1}) = F\chi_i(t_{k-1}), \quad i = 0, 1, \dots, 2L. \quad (21)$$

The weighted mean of these predicted sigma points for the augmented state is given by

$$\hat{X}^-(t_k) = \sum_{i=0}^{2L} W_i^m \chi_i(t_k | t_{k-1}), \quad (22)$$

where  $W_0^m = \lambda / (L + \lambda)$ ,  $W_i^m = 1 / \{2(L + \lambda)\}$ ,  $i = 1, 2, \dots, 2L$ .

From (21) and (22), the covariance matrix of the augmented state can be predicted as,

$$P^-(t_k) = \sum_{i=0}^{2L} W_i^c [\chi_i(t_k | t_{k-1}) - \hat{X}^-(t_k)][\chi_i(t_k | t_{k-1}) - \hat{X}^-(t_k)]^T + R_X, \quad (23)$$

where  $W_0^c = \lambda / (L + \lambda) + (1 - \alpha^2 + \beta)$  and  $W_i^c = 1 / \{2(L + \lambda)\}$ ,  $i = 1, 2, \dots, 2L$ . Matrix  $R_X$  is a combined

covariance given by  $R_X = \begin{bmatrix} R_{target} & \mathbf{0} & \mathbf{0} \\ \mathbf{0} & R_{ESM} & \mathbf{0} \\ \mathbf{0} & \mathbf{0} & I \end{bmatrix}$ . For a constant-velocity target,

$$R_{target} = \delta_\mu^2 \begin{bmatrix} T^3/3 & T^2/2 \\ T^2/2 & T \end{bmatrix} \text{ and } R_{ESM} = \delta_v^2 \begin{bmatrix} T^3/3 & T^2/2 \\ T^2/2 & T \end{bmatrix}.$$

Given the weighted sigma points  $\hat{X}^-(t_k)$  and the predicted covariance matrix of the state  $P^-(t_k)$ , we recompute the sigma points using (20). Let  $\chi_i^r(t_k | t_{k-1})$ ,  $i = 0, 1, \dots, 2L$ , denote the new sigma points, the prediction of sigma points for the measurements becomes

$$Z_i^-(t_k | t_{k-1}) = h(\chi_i^r(t_k | t_{k-1})), \quad (24)$$

and the weighted mean of these sigma points can be obtained as

$$\hat{Z}^-(t_k) = \sum_{i=0}^{2L} W_i^m Z_i^-(t_k | t_{k-1}). \quad (25)$$

The covariance matrix of the predicted observations is given by

$$P_{zz}(t_k) = \sum_{i=0}^{2L} W_i^c [Z_i^-(t_k | t_{k-1}) - \hat{Z}^-(t_k)][Z_i^-(t_k | t_{k-1}) - \hat{Z}^-(t_k)]^T + R_z, \quad (26)$$

where  $R_z$  is the covariance matrix of the measurement noise. The covariance matrix between the states and measurements are updated by

$$P_{xz}(t_k) = \sum_{i=0}^{2L} W_i^c [\chi_i^r(t_k | t_{k-1}) - \hat{X}^-(t_k)][Z_i^-(t_k | t_{k-1}) - \hat{Z}^-(t_k)]^T. \quad (27)$$

With  $\mathbf{P}_{zz}$  and  $\mathbf{P}_{xz}$ , the Kalman filter gain can be determined by

$$\mathbf{G}(t_k) = \mathbf{P}_{xz}(t_k)\mathbf{P}_{zz}^{-1}(t_k), \quad (28)$$

and the augmented state estimate  $\hat{\mathbf{X}}(t_k)$  and its covariance matrix can be updated by

$$\hat{\mathbf{X}}(t_k) = \hat{\mathbf{X}}^-(t_k) + \mathbf{G}(t_k)[\mathbf{Z}(t_k) - \hat{\mathbf{Z}}^-(t_k)] \quad (29)$$

$$\mathbf{P}(t_k) = \mathbf{P}^-(t_k) - \mathbf{G}(t_k)\mathbf{P}_{zz}(t_k)\mathbf{G}^T(t_k). \quad (30)$$

The stability of the UKF comes from its so-called “unscented transformation”. It is known that the optimality of the Kalman estimator relies on the Gaussian assumption about the state vector. In the EKF, the distribution of the state is approximated by a Gaussian distribution and propagated analytically through a first-order linearization of the nonlinear system. This could introduce large errors in the posteriori mean and covariance of the transformed states, making the EKF sub-optimal and often divergent. The UKF addresses the approximation problem using a different approach. The distribution of the state now is represented by a set of selected sampling points. These sampling points are able to capture the posterior mean and covariance of the state accurately to the third order. Compared to the EKF that only uses a first-order approximation, the UKF is able to provide more accurate and stable state estimates. However, the trade-off is the computation complexity introduced in the UKF.

## 4. Performance Analysis

In this section, we analyze the performance of the proposed UKF registration algorithm for mobile radar and ESM sensors. The registration performance is assessed using the PCRB. The effect of the registration error on the target state estimates is discussed. The robustness of the proposed algorithm is also looked into using the sensitivity analysis.

### 4.1 Derivation of the PCRB

Given  $\mathcal{S}_l(t_k) = \{s_l(t_1), s_l(t_2), \dots, s_l(t_k)\}$ ,  $l = 1, 2, \dots, 2^k$ , for the ESM sensor at time  $t_k$ , the covariance of an unbiased state estimate  $\hat{\mathbf{X}}(t_k)$  has the following lower bound:

$$E \left\{ \left[ \hat{\mathbf{X}}(t_k) - \mathbf{X}(t_k) \right] \left[ \hat{\mathbf{X}}(t_k) - \mathbf{X}(t_k) \right]^T \middle| \mathcal{S}_l(t_k) \right\} \geq \left[ \mathbf{J}_{t_k}(\mathcal{S}_l(t_k)) \right]^{-1}, \quad (31)$$

where the  $ij$  th element of the Fisher information matrix is given by

$$\mathbf{J}_{ij} = E \left\{ - \frac{\partial^2 p(\mathbf{X}(t_k), \mathbf{Z}(t_k) | \mathcal{S}_l(t_k))}{\partial \mathbf{X}(t_k) \partial \mathbf{Z}(t_k)} \right\}. \quad (32)$$

The PCRB  $\mathbf{C}(\mathcal{S}_l(t_k))$  is defined as

$$\mathbf{C}(\mathcal{S}_l(t_k)) = \left[ \mathbf{J}_{t_k}(\mathcal{S}_l(t_k)) \right]^{-1}. \quad (33)$$

Since the system biases in the augmented state are constants, the conditional distribution of  $\mathbf{X}(t_{k+1})$ , given  $\mathbf{X}(t_k)$ , is singular [27]. The augmented state equation (16) can be divided into two parts

$$\begin{aligned} \mathbf{X}^{(1)}(t_{k+1}) &= \mathbf{F}_1 \mathbf{X}^{(1)}(t_k) + \mathbf{n}_{X^{(1)}}(t_k) \\ \mathbf{X}^{(2)}(t_{k+1}) &= \mathbf{X}^{(2)}(t_k), \end{aligned} \quad (34)$$

where

$$\mathbf{X}^{(1)}(t_k) = [\zeta^T(t_k), \psi^T(t_k)]^T, \quad \mathbf{X}^{(2)}(t_k) = [\Delta t, \Delta \theta_R, \Delta r_R, \Delta \theta_E]^T, \quad \mathbf{n}_{X^{(1)}}(t_k) = [\Gamma \mu(t_k), \Gamma \nu(t_k)]^T \quad \text{and}$$

$\mathbf{F}_1 = \begin{bmatrix} \Phi & \mathbf{0} \\ \mathbf{0} & \Phi \end{bmatrix}$ . The dimension  $L_2$  of  $\mathbf{X}^{(2)}(t_k)$  is 4, and the dimension  $L_1$  of  $\mathbf{X}^{(1)}(t_k)$  is 8 and 12 for the constant-velocity and constant-acceleration model, respectively. The dimension of the augmented state vector is given by  $L_1 + L_2 = L$ .

To derive an explicit formula for the Fisher information matrix, we define the following probability density function  $\bar{p}(t_k)$

$$\begin{aligned} \bar{p}(t_k) = & p\left(\mathbf{X}^{(1)}(t_{k+1}) \middle| \mathbf{X}^{(1)}(t_k), \mathbf{S}_l(t_{k+1})\right) \\ & \cdot p\left(\mathbf{Z}(t_{k+1}) \middle| \mathbf{X}^{(1)}(t_k), \mathbf{X}^{(2)}(t_k), \mathbf{X}^{(1)}(t_{k+1}), \mathbf{S}_l(t_{k+1})\right) \end{aligned} \quad (35)$$

From (34) and (17), we can obtain the two probability density functions in (35) as follows [29]:

$$\begin{aligned} p\left(\mathbf{X}^{(1)}(t_{k+1}) \middle| \mathbf{X}^{(1)}(t_k), \mathbf{S}_l(t_{k+1})\right) &= p\left(\mathbf{X}^{(1)}(t_{k+1}) \middle| \mathbf{X}^{(1)}(t_k)\right) \\ &= \frac{1}{\sqrt{2\pi} \det(\mathbf{R}_{\mathbf{X}^{(1)}})} \exp\{-[\mathbf{X}^{(1)}(t_{k+1}) - \mathbf{F}_1 \mathbf{X}^{(1)}(t_k)]^T \mathbf{R}_{\mathbf{X}^{(1)}}^{-1} [\mathbf{X}^{(1)}(t_{k+1}) - \mathbf{F}_1 \mathbf{X}^{(1)}(t_k)]\}, \end{aligned} \quad (36)$$

and

$$\begin{aligned} p\left(\mathbf{Z}(t_{k+1}) \middle| \mathbf{X}^{(1)}(t_k), \mathbf{X}^{(2)}(t_k), \mathbf{X}^{(1)}(t_{k+1}), \mathbf{S}_l(t_{k+1})\right) &= \frac{1}{\sqrt{2\pi} \det(\mathbf{R}_z)} \\ &\cdot \exp\{[\mathbf{Z}(t_{k+1}) - \mathbf{h}(\mathbf{X}^{(1)}(t_k), \mathbf{X}^{(2)}(t_k), \mathbf{X}^{(1)}(t_{k+1}), \mathbf{S}_l(t_{k+1}))]\mathbf{R}_z^{-1} \\ &\quad [\mathbf{Z}(t_{k+1}) - \mathbf{h}(\mathbf{X}^{(1)}(t_k), \mathbf{X}^{(2)}(t_k), \mathbf{X}^{(1)}(t_{k+1}), \mathbf{S}_l(t_{k+1}))]\}^T \}. \end{aligned} \quad (37)$$

From (36) and (37), we can obtain the derivatives of  $\bar{p}(t_k)$ ,

$$\bar{\mathbf{H}}_{11}(t_k) = E \left\{ \frac{\partial^2 \bar{p}(t_k)}{\partial \mathbf{X}^{(1)}(t_k) \partial \mathbf{X}^{(1)}(t_k)} \right\} = \mathbf{F}_1^T \mathbf{R}_{\mathbf{X}^{(1)}}^{-1} \mathbf{F}_1 \quad (38)$$

$$\bar{\mathbf{H}}_{12}(t_k) = E \left\{ \frac{\partial^2 \bar{p}(t_k)}{\partial \mathbf{X}^{(1)}(t_k) \partial \mathbf{X}^{(2)}(t_k)} \right\} = \mathbf{0} \quad (39)$$

$$\bar{\mathbf{H}}_{13}(t_k) = E \left\{ \frac{\partial^2 \bar{p}(t_k)}{\partial \mathbf{X}^{(1)}(t_k) \partial \mathbf{X}^{(1)}(t_{k+1})} \right\} = \mathbf{F}_1^T \mathbf{R}_{\mathbf{X}^{(1)}}^{-1} \quad (40)$$

$$\bar{\mathbf{H}}_{22}(t_k) = E \left\{ \frac{\partial^2 \bar{p}(t_k)}{\partial \mathbf{X}^{(2)}(t_k) \partial \mathbf{X}^{(2)}(t_k)} \right\} = E \{ \mathbf{H}_2^T(t_k) \mathbf{R}_z^{-1} \mathbf{H}_2^T(t_k) \} \quad (41)$$

$$\bar{\mathbf{H}}_{23}(t_k) = E \left\{ \frac{\partial^2 \bar{p}(t_k)}{\partial \mathbf{X}^{(1)}(t_{k+1}) \partial \mathbf{X}^{(2)}(t_k)} \right\} = E \{ \mathbf{H}_1^T(t_k) \mathbf{R}_z^{-1} \mathbf{H}_2^T(t_k) \} \quad (42)$$

$$\bar{\mathbf{H}}_{33}(t_k) = E \left\{ \frac{\partial^2 \bar{p}(t_k)}{\partial \mathbf{X}^{(1)}(t_{k+1}) \partial \mathbf{X}^{(1)}(t_{k+1})} \right\} = \mathbf{R}_{\mathbf{X}^{(1)}}^{-1} + E \{ \mathbf{H}_2^T(t_k) \mathbf{R}_z^{-1} \mathbf{H}_1^T(t_k) \}, \quad (43)$$

where  $\mathbf{H}_1(t_k)$  and  $\mathbf{H}_2(t_k)$  are defined by

$$\mathbf{H}_1(t_k) = \frac{\partial \left( \mathbf{h}(\mathbf{X}^{(1)}(t_k), \mathbf{X}^{(2)}(t_k), \mathbf{X}^{(1)}(t_{k+1}), \mathbf{S}_l(t_{k+1})) \right)}{\partial \mathbf{X}^{(1)}(t_{k+1})},$$



$$\mathbf{H}_2(t_k) = \frac{\partial \left( \mathbf{h}(\mathbf{X}^{(1)}(t_k), \mathbf{X}^{(2)}(t_k), \mathbf{X}^{(1)}(t_{k+1}), \mathbf{S}_l(t_{k+1})) \right)}{\partial \mathbf{X}^{(2)}(t_k)}.$$

The detailed computation of  $\mathbf{H}_1(t_k)$  and  $\mathbf{H}_2(t_k)$  are given in Annex B.

Finally, the Fisher information matrix can be written in a block matrix form,

$$\mathbf{J}(t_k) = \begin{bmatrix} \mathbf{J}_{11}(t_k) & \mathbf{J}_{12}(t_k) \\ \mathbf{J}_{21}(t_k) & \mathbf{J}_{22}(t_k) \end{bmatrix}. \quad (44)$$

Using the derivatives in (38) ~ (43), we can obtain the similar explicit formulas for the block matrix as [26]

$$\mathbf{J}_{11}(t_{k+1}) = \bar{\mathbf{H}}_{33}(t_k) - [\bar{\mathbf{H}}_{13}(t_k)]^T [\mathbf{J}_{11}(t_k) + \bar{\mathbf{H}}_{11}(t_k)]^{-1} \bar{\mathbf{H}}_{13}(t_k) \quad (45)$$

$$\mathbf{J}_{12}(t_{k+1}) = \mathbf{J}_{21}^T(t_{k+1}) = [\bar{\mathbf{H}}_{23}(t_k)]^T - [\bar{\mathbf{H}}_{13}(t_k)]^T [\mathbf{J}_{11}(t_k) + \bar{\mathbf{H}}_{11}(t_k)]^{-1} \mathbf{J}_{12}(t_k) \quad (46)$$

$$\mathbf{J}_{22}(t_{k+1}) = \mathbf{J}_{22}(t_k) + \bar{\mathbf{H}}_{22}(t_k) - [\mathbf{J}_{12}(t_k)]^T [\mathbf{J}_{11}(t_k) + \bar{\mathbf{H}}_{11}(t_k)]^{-1} \mathbf{J}_{12}(t_k). \quad (47)$$

The PCRB of the mobile radar/ESM registration problem can then be obtained by using (32).

## 4.2 Effects of sensor biases on target state estimates

The performance of radar/ESM systems is affected by the space-time system biases. We will examine the estimation errors of the target states with and without space-time alignment, and show that the target state estimates are unbiased if the space-time system biases are aligned correctly. Let  $\boldsymbol{\eta} = [\Delta t, \Delta \theta_R, \Delta r_R, \Delta \theta_E]^T$  denote the space-time system biases. Equation (17) can be rewritten as

$$\mathbf{Z}(t_k) = \mathbf{h}_1(\mathbf{X}^{(1)}(t_k)) + \mathbf{h}_2(\mathbf{X}^{(1)}(t_k), \boldsymbol{\eta}) + \mathbf{n}_z(t_k), \quad (48)$$

where

$$\mathbf{h}_1(\mathbf{X}^{(1)}(t_k)) = [x_R(t_k), y_R(t_k), \text{artg} \left( \frac{x_R(t_k) - u(t_k)}{y_R(t_k) - v(t_k)} \right), u(t_k), v(t_k)]^T \quad (49)$$

$$\begin{aligned}
\mathbf{h}_2(\mathbf{X}^{(1)}(t_k), \boldsymbol{\eta}) &= [\dot{x}_R(t_k)\Delta t + y_R(t_k)\Delta\theta_R + \frac{x_R(t_k)}{\sqrt{x_R^2(t_k) + y_R^2(t_k)}}\Delta r_R, \\
&\dot{y}_R(t_k)\Delta t - x_R(t_k)\Delta\theta_R + \frac{y_R(t_k)}{\sqrt{x_R^2(t_k) + y_R^2(t_k)}}\Delta r_R, \\
&\Delta\theta_E, \quad \dot{u}(t_k)\Delta t + v(t_k)\Delta\theta_R + \frac{u(t_k)}{\sqrt{u^2(t_k) + v^2(t_k)}}\Delta r_R, \\
&\dot{v}(t_k)\Delta t - u(t_k)\Delta\theta_R + \frac{v(t_k)}{\sqrt{u^2(t_k) + v^2(t_k)}}\Delta r_R]^T.
\end{aligned} \tag{50}$$

Based on the state equation (34) and the above measurement equation, the estimation error of the target state  $\mathbf{X}^{(1)}(t_k)$  with space-time alignment can be written as

$$\begin{aligned}
\mathbf{e}_1(t_k) &= \hat{\mathbf{X}}^{(1)}(t_k) - \mathbf{X}^{(1)}(t_k) \\
&= [\hat{\mathbf{X}}^-(t_k) + \mathbf{G}(t_k)(\mathbf{Z}(t_k) - \hat{\mathbf{Z}}^-(t_k))] - [\mathbf{F}_1\mathbf{X}^{(1)}(t_{k-1}) + \mathbf{n}_{\mathbf{X}^{(1)}}(t_k)] \\
&= \mathbf{F}_1\mathbf{e}_1(t_{k-1}) + \mathbf{G}(t_k)\mathbf{n}_z(t_k) - \mathbf{n}_{\mathbf{X}^{(1)}}(t_{k-1}) \\
&\quad + \mathbf{G}(t_k)[\mathbf{h}_1(\mathbf{X}^{(1)}(t_k)) + \mathbf{h}_2(\mathbf{X}^{(1)}(t_k), \boldsymbol{\eta}) - \mathbf{h}_1(\hat{\mathbf{X}}^{(1)-}(t_k)) - \mathbf{h}_2(\hat{\mathbf{X}}^{(1)-}(t_k), \boldsymbol{\eta})].
\end{aligned} \tag{51}$$

Using a first-order approximation, (51) becomes

$$\mathbf{e}_1(t_k) = [\mathbf{I} - \mathbf{G}(t_k)\bar{\boldsymbol{\Gamma}}(t_k)]\mathbf{F}_1\mathbf{e}_1(t_{k-1}) + \mathbf{G}(t_k)\mathbf{n}_z(t_k) - \mathbf{n}_{\mathbf{X}^{(1)}}(t_{k-1}) \tag{52}$$

where  $\bar{\boldsymbol{\Gamma}}(t_k) = \partial(\mathbf{h}_1(\mathbf{X}^{(1)}(t_k)) + \mathbf{h}_2(\mathbf{X}^{(1)}(t_k), \boldsymbol{\eta})) / \partial\mathbf{X}^{(1)}(t_k)$ . Substituting  $\mathbf{e}_1(t_{k-i})$  into (52) yields

$$\begin{aligned}
\mathbf{e}_1(t_k) &= \left[ \prod_{i=2}^k (\mathbf{I} - \mathbf{G}(t_i)\bar{\boldsymbol{\Gamma}}(t_i))\mathbf{F}_1 \right] \mathbf{e}_1(t_1) \\
&\quad + \sum_{j=2}^k \left[ \prod_{i=j+1}^k (\mathbf{I} - \mathbf{G}(t_i)\bar{\boldsymbol{\Gamma}}(t_i))\mathbf{F}_1 \right] [\mathbf{G}(t_j)\mathbf{n}_z(t_j) - \mathbf{n}_{\mathbf{X}^{(1)}}(t_{j-1})].
\end{aligned} \tag{53}$$

Assume that that  $\mathbf{e}_1(t_1)$ ,  $\mathbf{n}_z(t_k)$  and  $\mathbf{n}_{\mathbf{X}^{(1)}}(t_k)$  are all zero mean white Gaussian processes. The expectation of  $\mathbf{e}_1(t_k)$  can be obtained as

$$\begin{aligned}
E\{\mathbf{e}_1(t_k)\} &= \left[ \prod_{i=2}^k (\mathbf{I} - \mathbf{G}(t_i)\bar{\boldsymbol{\Gamma}}(t_i))\mathbf{F}_1 \right] E\{\mathbf{e}_1(t_1)\} \\
&\quad + \sum_{j=2}^k \left[ \prod_{i=j+1}^k (\mathbf{I} - \mathbf{G}(t_i)\bar{\boldsymbol{\Gamma}}(t_i))\mathbf{F}_1 \right] [\mathbf{G}(t_j)E\{\mathbf{n}_z(t_j)\} - E\{\mathbf{n}_{\mathbf{X}^{(1)}}(t_{j-1})\}] = \mathbf{0},
\end{aligned} \tag{54}$$

indicating that the state estimate of the target by the UKF is unbiased if the space-time system biases are corrected.

When the sensors are not aligned, the estimation error of the target state is given by

$$\begin{aligned} \mathbf{e}_2(t_k) &= \hat{\mathbf{X}}^{(1)}(t_k) - \mathbf{X}^{(1)}(t_k) \\ &= \mathbf{F}_1 \mathbf{e}_1(t_{k-1}) + \mathbf{G}(t_k) \mathbf{n}_z(t_k) - \mathbf{n}_{\mathbf{X}^{(1)}}(t_{k-1}) \\ &\quad + \mathbf{G}(t_k) [\mathbf{h}_1(\mathbf{X}^{(1)}(t_k)) - \mathbf{h}_1(\hat{\mathbf{X}}^{(1)}(t_k))] + \mathbf{G}(t_k) \mathbf{h}_2(\mathbf{X}^{(1)}(t_k), \boldsymbol{\eta}). \end{aligned} \quad (55)$$

Using a first-order approximation, (55) becomes

$$\begin{aligned} \mathbf{e}_2(t_k) &= [\mathbf{I} - \mathbf{G}(t_k) \bar{\mathbf{F}}_1(t_k)] \mathbf{F}_1 \mathbf{e}_2(t_{k-1}) \\ &\quad + \mathbf{G}(t_k) \mathbf{n}_z(t_k) - \mathbf{n}_{\mathbf{X}^{(1)}}(t_{k-1}) + \mathbf{G}(t_k) \mathbf{h}_2(\mathbf{X}^{(1)}(t_k), \boldsymbol{\eta}) \end{aligned} \quad (56)$$

where  $\bar{\mathbf{F}}_1(t_k) = \partial(\mathbf{h}_1(\mathbf{X}^{(1)}(t_k))) / \partial \mathbf{X}^{(1)}(t_k)$ . Similarly, substituting  $\mathbf{e}_2(t_{k-i})$  into (56), we have

$$\begin{aligned} \mathbf{e}_2(t_k) &= \left[ \prod_{i=2}^k (\mathbf{I} - \mathbf{G}(t_i) \bar{\mathbf{F}}_1(t_i)) \mathbf{F}_1 \right] \mathbf{e}_2(t_1) \\ &\quad + \sum_{j=2}^k \left[ \prod_{i=j+1}^k (\mathbf{I} - \mathbf{G}(t_i) \bar{\mathbf{F}}_1(t_i)) \mathbf{F}_1 \right] \left[ \mathbf{G}(t_j) \mathbf{n}_z(t_j) - \mathbf{n}_{\mathbf{X}^{(1)}}(t_{j-1}) \right] \\ &\quad + \sum_{j=2}^k \left[ \prod_{i=j+1}^k (\mathbf{I} - \mathbf{G}(t_i) \bar{\mathbf{F}}_1(t_i)) \mathbf{F}_1 \right] \left[ \mathbf{G}(t_j) \mathbf{h}_2(\mathbf{X}^{(1)}(t_j), \boldsymbol{\eta}) \right]. \end{aligned} \quad (57)$$

When  $\mathbf{e}_2(t_1)$ ,  $\mathbf{n}_z(t_k)$  and  $\mathbf{n}_{\mathbf{X}^{(1)}}(t_k)$  are assumed to be zero mean white Gaussian processes, the expectation of  $\mathbf{e}_2(t_k)$  can be obtained as

$$E \{ \mathbf{e}_2(t_k) \} = \sum_{j=2}^k \left[ \prod_{i=j+1}^k (\mathbf{I} - \mathbf{G}(t_i) \bar{\mathbf{F}}_1(t_i)) \mathbf{F}_1 \right] \left[ \mathbf{G}(t_j) \mathbf{h}_2(\mathbf{X}^{(1)}(t_j), \boldsymbol{\eta}) \right]. \quad (58)$$

It can be seen from (58) that, when the sensors are not aligned properly, the sensor bias estimates are no longer zero, i.e., in the presence of sensor biases, the target state estimates are biased. In addition, the larger the space-time system biases  $\boldsymbol{\eta}$ , the larger the biases of the target state estimate.

### 4.3 Sensitivity Analysis

Sensitivity analysis is a popular method to analyze the robustness performance of an estimator [30]. We

first analyze the sensitivity of the Jacobian matrix  $\mathbf{H}(t_k) = \frac{\partial \mathbf{Z}(t_k)}{\partial \mathbf{X}(t_k)}$  on the performance of the state

estimates by the EKF. Let  $\Delta \mathbf{H}(t_k) = \mathbf{H}^*(t_k) - \mathbf{H}(t_k)$  denote the perturbation of the Jacobian matrix  $\mathbf{H}(t_k)$ , then the Kalman gain of the EKF in (70) (Annex A) is given by

$$\begin{aligned}
\mathbf{G}^*(t_k) &= \mathbf{P}^-(t_k) \mathbf{H}^*(t_k) [\mathbf{H}^*(t_k) \mathbf{P}^-(t_k) \mathbf{H}^{*T}(t_k) + \mathbf{R}_z]^{-1} \\
&= \mathbf{P}^-(t_k) [\mathbf{H}(t_k) + \Delta \mathbf{H}(t_k)] \\
&\quad \cdot \left\{ [\mathbf{H}(t_k) + \Delta \mathbf{H}(t_k)] \mathbf{P}^-(t_k) [\mathbf{H}^T(t_k) + \Delta \mathbf{H}^T(t_k)] + \mathbf{R}_z \right\}^{-1}.
\end{aligned} \tag{59}$$

Because  $[\mathbf{A} + \Delta \mathbf{A}]^{-1} = \mathbf{A}^{-1} + \mathbf{A}^{-1} \Delta \mathbf{A} \mathbf{A}^{-1}$ , we have

$$\mathbf{G}^*(t_k) = \mathbf{P}^-(t_k) [\mathbf{H}(t_k)]^T [\mathbf{H}(t_k) \mathbf{P}^-(t_k) \mathbf{H}^T(t_k)] + \Delta \mathbf{B}, \tag{60}$$

where

$$\Delta \mathbf{B} = \mathbf{P}^-(t_k) \left\{ \mathbf{H}^T(t_k) \Delta \mathbf{A} + \Delta \mathbf{H}^T(t_k) [\mathbf{H}(t_k) \mathbf{P}^{-1}(t_k) + \mathbf{R}_z]^{-1} + \Delta \mathbf{H}^T(t_k) \Delta \mathbf{A} \right\} \tag{61}$$

$$\begin{aligned}
\Delta \mathbf{A} &= [\mathbf{H}(t_k) \mathbf{P}^-(t_k) \mathbf{H}^T(t_k)]^{-1} [\mathbf{H}(t_k) \mathbf{P}^-(t_k) \Delta \mathbf{H}^T(t_k) + \Delta \mathbf{H}(t_k) \mathbf{P}^-(t_k) \mathbf{H}^T(t_k)] \\
&\quad + \Delta \mathbf{H}(t_k) \mathbf{P}^-(t_k) \Delta \mathbf{H}^T(t_k) ]^{-1} [\mathbf{H}(t_k) \mathbf{P}^-(t_k) \mathbf{H}^T(t_k)]^{-1}.
\end{aligned} \tag{62}$$

Then the covariance matrix of the state estimation error defined in (71) is given by

$$\begin{aligned}
\mathbf{P}^*(t_k) &= [\mathbf{I} - \mathbf{G}^*(t_k) \mathbf{H}^*(t_k)] \mathbf{P}^-(t_k) \\
&= \mathbf{P}^-(t_k) - \mathbf{P}^-(t_k) \mathbf{H}^T(t_k) [\mathbf{H}(t_k) \mathbf{P}^{-1}(t_k) \mathbf{H}^T(t_k) + \mathbf{R}_z]^{-1} \mathbf{H}(t_k) \mathbf{P}^-(t_k) \\
&\quad - \mathbf{P}^{-1}(t_k) \mathbf{H}^T(t_k) \Delta \mathbf{B} \mathbf{H}(t_k) \mathbf{P}^{-1}(t_k) - \mathbf{G}^*(t_k) \Delta \mathbf{H}(t_k) \mathbf{P}^{-1}(t_k).
\end{aligned} \tag{63}$$

Equations (61) and (63) show that the perturbation  $\Delta \mathbf{H}(t_k)$  of the Jacobian contributes to the covariance of the state estimate by

$$\Delta \mathbf{P}(t_k) = \mathbf{P}^{-1}(t_k) \mathbf{H}^T(t_k) \Delta \mathbf{B} \mathbf{H}(t_k) \mathbf{P}^{-1}(t_k) + \mathbf{G}^*(t_k) \Delta \mathbf{H}(t_k) \mathbf{P}^{-1}(t_k)$$

and the Kalman gain by  $\Delta \mathbf{B}$ . In the next section, it will be shown by simulations that for some track patterns, if  $\Delta \mathbf{P}(t_k)$  is too large, it may cause the EKF to diverge.

The sensitivity of the UKF is related to the unscented transformation. Assume that the prior variable  $\mathbf{X}$  is being perturbed by a zero-mean disturbance  $\delta \mathbf{X}$  with covariance  $\mathbf{P}_X$ . For the nonlinear measurement function  $\mathbf{Z} = \mathbf{h}(\mathbf{X})$ , the predicted mean and covariance by the unscented transformation are [22]

$$\bar{\mathbf{Z}} = \mathbf{h}(\bar{\mathbf{X}}) + \frac{1}{2} \left[ (\nabla^T \mathbf{P}_X \nabla) \mathbf{h}(\mathbf{X}) \right]_{\mathbf{X}=\bar{\mathbf{X}}} + \mathbf{O}_m(\delta \mathbf{X}), \tag{64}$$

and

$$\mathbf{P}_Z = \mathbf{H} \mathbf{P}_X \mathbf{H} - \frac{1}{4} \left\{ \left[ (\nabla^T \mathbf{P}_X \nabla) \mathbf{h}(\mathbf{X}) \right] \left[ (\nabla^T \mathbf{P}_X \nabla) \mathbf{h}(\mathbf{X}) \right]^T \right\}_{\mathbf{X}=\bar{\mathbf{X}}} + \mathbf{O}_c(\delta \mathbf{X}), \tag{65}$$

where  $\mathbf{H}$  is the Jacobian matrix of  $\mathbf{h}(\mathbf{X})$  evaluated at  $\bar{\mathbf{X}}$ ,  $\mathbf{O}_m(\delta \mathbf{X})$  and  $\mathbf{O}_c(\delta \mathbf{X})$  represent the higher-order terms. The unscented transformation calculates the posterior mean and covariance to the first two terms with errors introduced only in the higher-order terms. By using a first-order approximation for

$\Delta \mathbf{H}(t_k) = \mathbf{H}^*(t_k) - \mathbf{H}(t_k)$ , we can obtain the perturbation  $\Delta \mathbf{G}(t_k) = \mathbf{G}^*(t_k) - \mathbf{G}(t_k)$  of the Kalman gain in the UKF from (28), (64) and (65) as

$$\Delta \mathbf{G}(t_k) = \mathbf{P}^-(t_k) \Delta \mathbf{H}^T(t_k) \mathbf{H}(t_k) \mathbf{P}^-(t_k) \mathbf{H}(t_k). \quad (66)$$

## 5. Experimental Results

In this section, the performance of the UKF-based registration algorithm for mobile radar and ESM sensors is evaluated. Both the constant-velocity and the constant-acceleration targets are considered. The performance is evaluated for ESM sensors of different detection probabilities. The radar is assumed to have a detection probability of one. In the following experiments, each trial is repeated 100 times to obtain the averaged results. The UKF parameters are chosen as  $\alpha = 1.0$ ,  $\beta = 2.0$ , and  $\kappa = 0.0$ .

### 5.1 Constant-velocity targets

We first consider the constant-velocity targets with different track patterns and ESM sensor detection probabilities. Three tracks and their corresponding radar measurements are shown in Figure 2(a). The fused tracks after registration are compared with the actual tracks in Figure 2(b). As we can see, the fused tracks are closer to the actual tracks than the radar measurements. This can be considered partial evidence that the system biases are corrected properly by the UKF registration algorithm. The detailed experimental results for one of the tracks are given below.

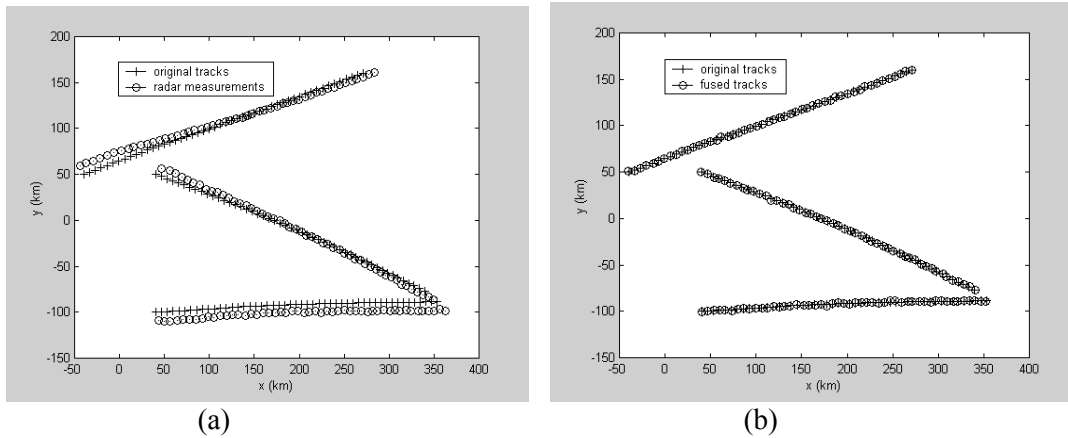


**Figure 2. Track plots of the constant-velocity targets. (a) actual tracks and the radar measurements; (b) actual and the fused tracks.**

Figures 3 and 4 show the mean square errors (MSEs) of the system bias estimates of the mobile radar and ESM sensors as well as the target state estimates of the constant-velocity target, respectively. The detection probability of the ESM sensor is set to 100%. The radar is located at (0,0). The parameters of the target states are given by initial position:  $(-40km, 50km)$ , initial velocity:  $(0.64km/s, 0.46km/s)$ ,

standard deviation of dynamics:  $\delta_\mu = 0.05 \text{ km}$ . The parameters of the ESM sensor states are given by initial position:  $(100\text{km}, 10\text{km})$ , initial velocity:  $(0.15\text{km/s}, 0.10\text{km/s})$ , and standard deviation of dynamics:  $\delta_\nu = 0.01 \text{ km}$ . The sampling interval  $T$  is  $10\text{s}$ . The radar and ESM sensor measurement noise variances are  $0.2 \text{ km}$  and  $0.002 \text{ rad}$ , respectively. The space-time system biases are given by:  $\Delta t = 0.2 \text{ s}$ ,  $\Delta\theta_R = 0.01 \text{ rad}$ ,  $\Delta r_R = 1.0 \text{ km}$ ,  $\Delta\theta_E = -0.01 \text{ rad}$ .

Figures 3(a) ~ 3(d) show the MSEs and PCRBs of the space-time system bias estimates versus the numbers of measurements. It is seen that the MSEs of the system bias estimates are close to the PCRBs, and the ratios of the MSEs to the actual biases are about 10% when the UKF is convergent. Figures 4(a) ~ 4(d) show the MSEs and PCRBs of the target state estimates versus the numbers of measurements. The MSEs of the fused target states are close to the PCRBs. As shown in Figures 4(a) and 4(b), when the number of measurements is 200, the radar measurement biases for the target positions along x- and y-axis are  $7.3\text{km}$  and  $11.2\text{km}$ , respectively while the MSEs of the target position estimates by the UKF are  $0.5\text{km}$  and  $1.1\text{km}$ , which means that the UKF registration algorithm has aligned the mobile sensor properly.

Figures 5 and 6 show the MSEs of the system bias estimates of the radar and ESM sensor and the state estimates of the constant-velocity target, respectively. The detection probability of the ESM sensor is set to 75%. In the range of  $k = 75 \sim 100$  and  $150 \sim 175$ , the ESM sensor is simulated to miss target. The other parameters are the same as the ones used in Figures 3 and 4. It is seen that the estimates of the system biases and the target states are close to the PCRBs when the ESM sensor detection probability is less than unity. When compared with the results of the unity detection probability for the ESM sensor, there is only small performance deterioration.

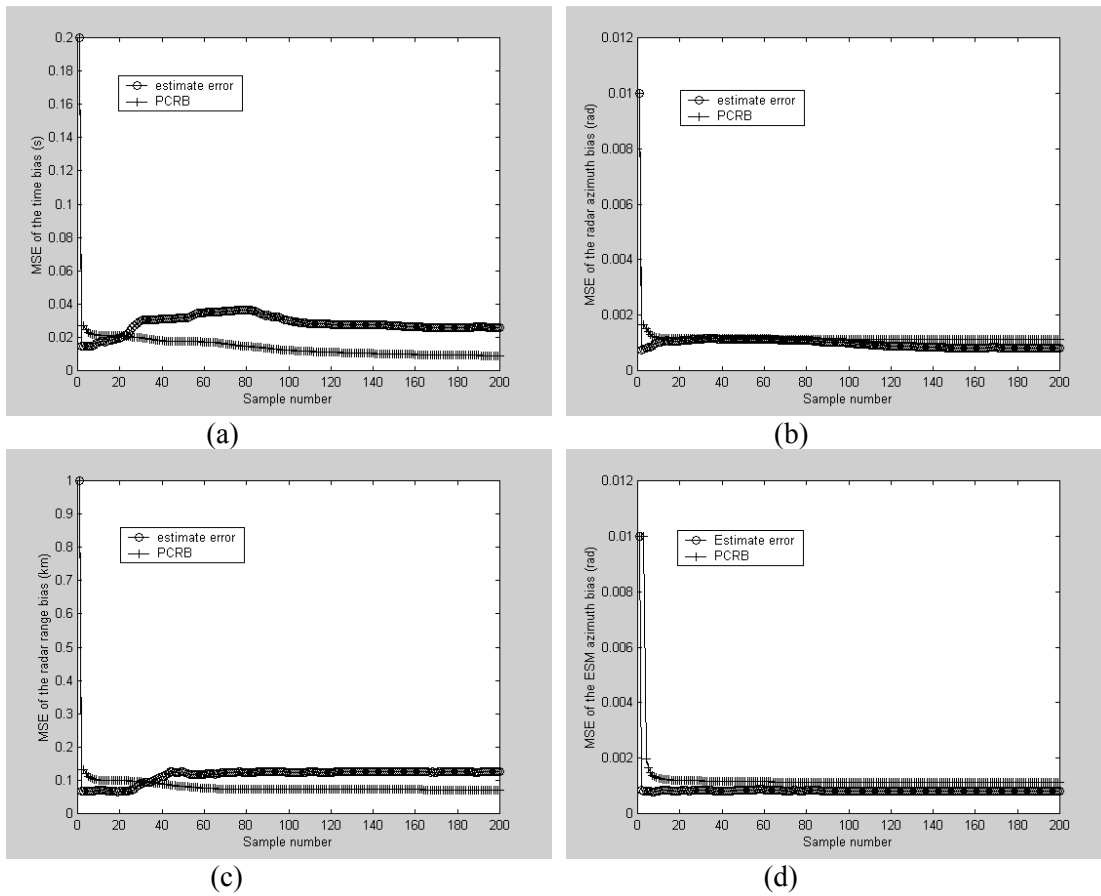


**Figure 3. Variation of the MSEs of the registration error estimates versus the number of measurements for the constant-velocity target and a unity detection probability for the ESM sensor: (a)  $\Delta t$ ; (b)  $\Delta\theta_R$ ; (c)  $\Delta r_R$ ; (d)  $\Delta\theta_E$ .**



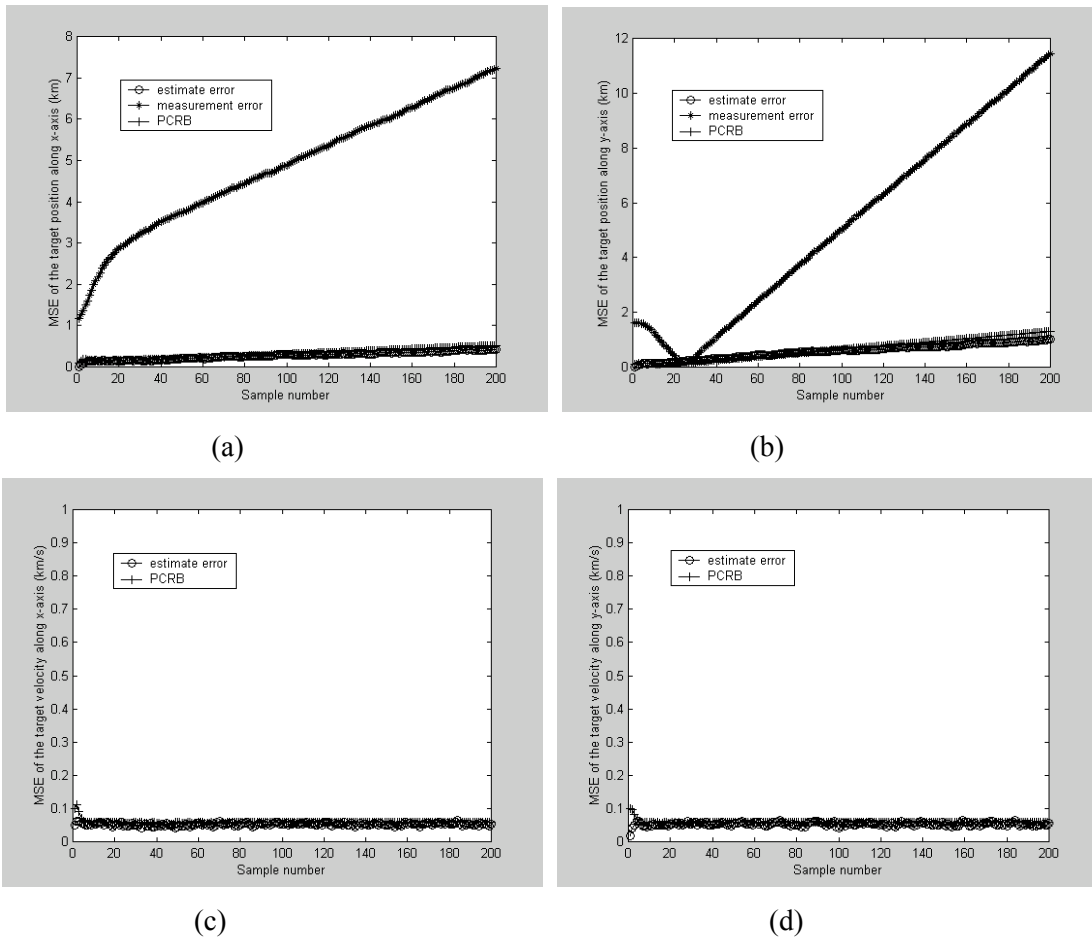


**Figure 4. Variation of the MSEs of the target state estimates versus the number of measurements for the constant-velocity state and a unity detection probability for the ESM sensor: (a) position along x-axis; (b) position along y-axis; (c) velocity along x-axis; (d) velocity along y-axis.**

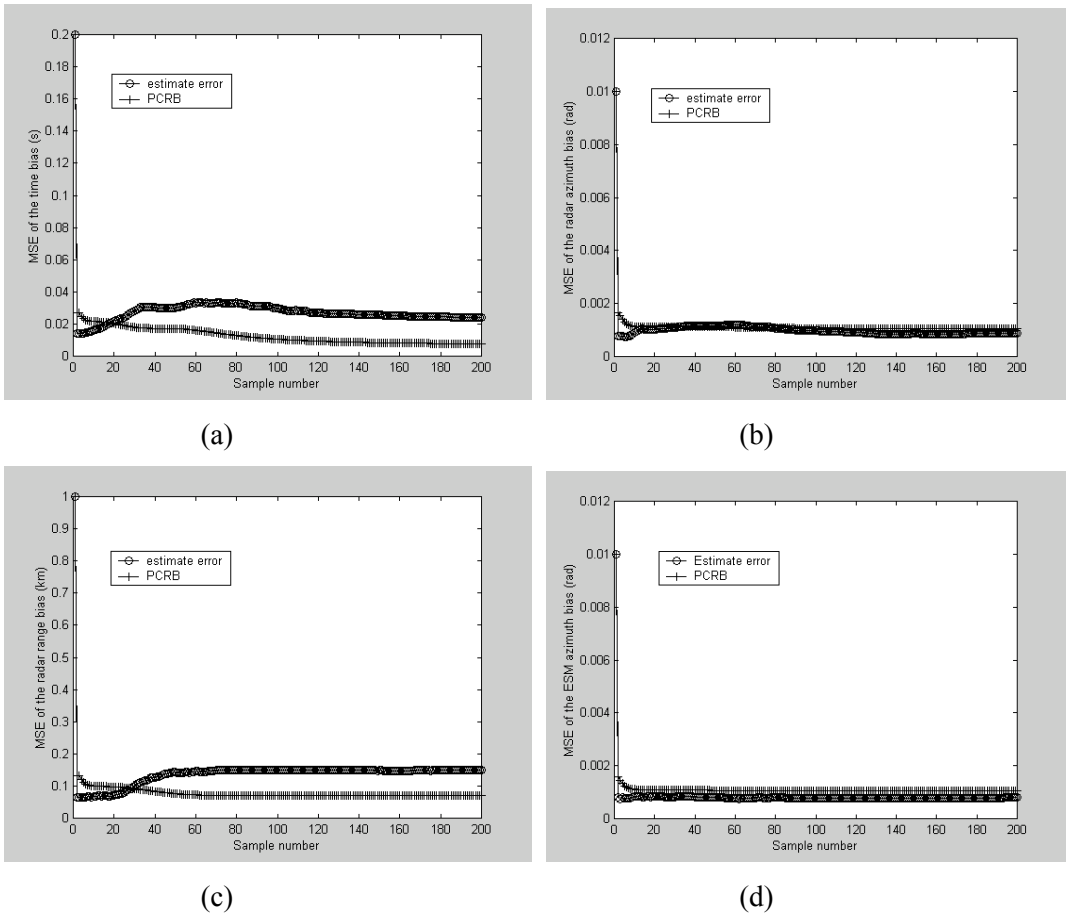
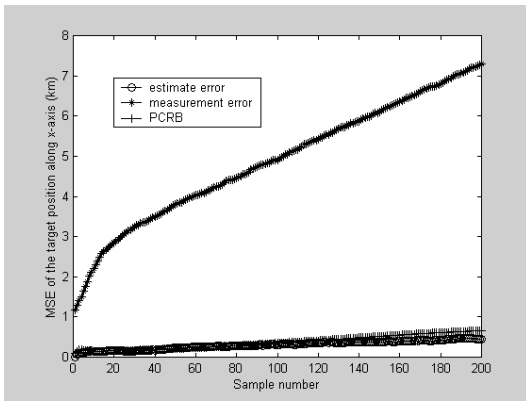
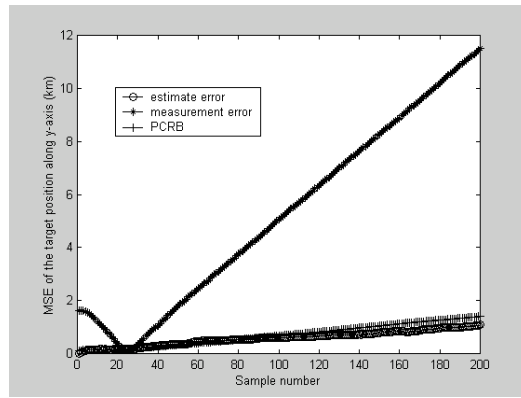


**Figure 5. Variation of the MSEs of the registration estimates versus the number of measurements for the constant-velocity target and a 75% detection probability for the ESM sensor: (a)  $\Delta t$ ; (b)  $\Delta\theta_R$ ; (c)  $\Delta r_R$ ; (d)**

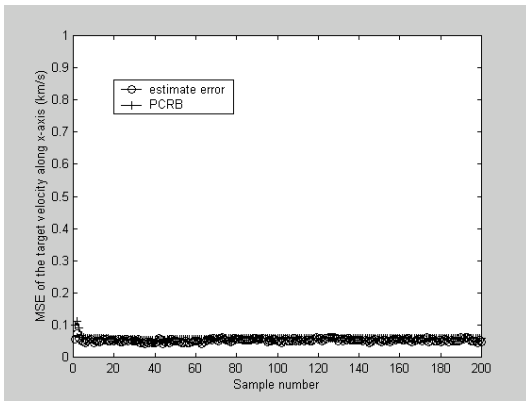
$\Delta\theta_E$ .



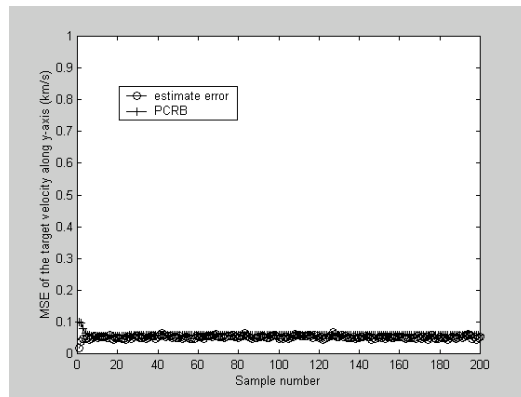
(a)



(b)



(c)



(d)

**Figure 6. Variation of the MSEs of the target state estimates versus the number of measurements for the constant-velocity target and a 75% detection probability for the ESM sensor: (a) position along x-axis; (b) position along y-axis; (c) velocity along x-axis; (d) velocity along y-axis.**

Figure 7 compares the target state estimates with and without measuring the ESM sensor states. If the motion of the ESM sensor with respect to the radar is not determined, the estimation error of the target states will deteriorate as shown in Figures 7(a) and 7(b), and the estimation error of the ESM positions caused by the system biases cannot be corrected successfully as shown in Figures 7(c) and 7(d).

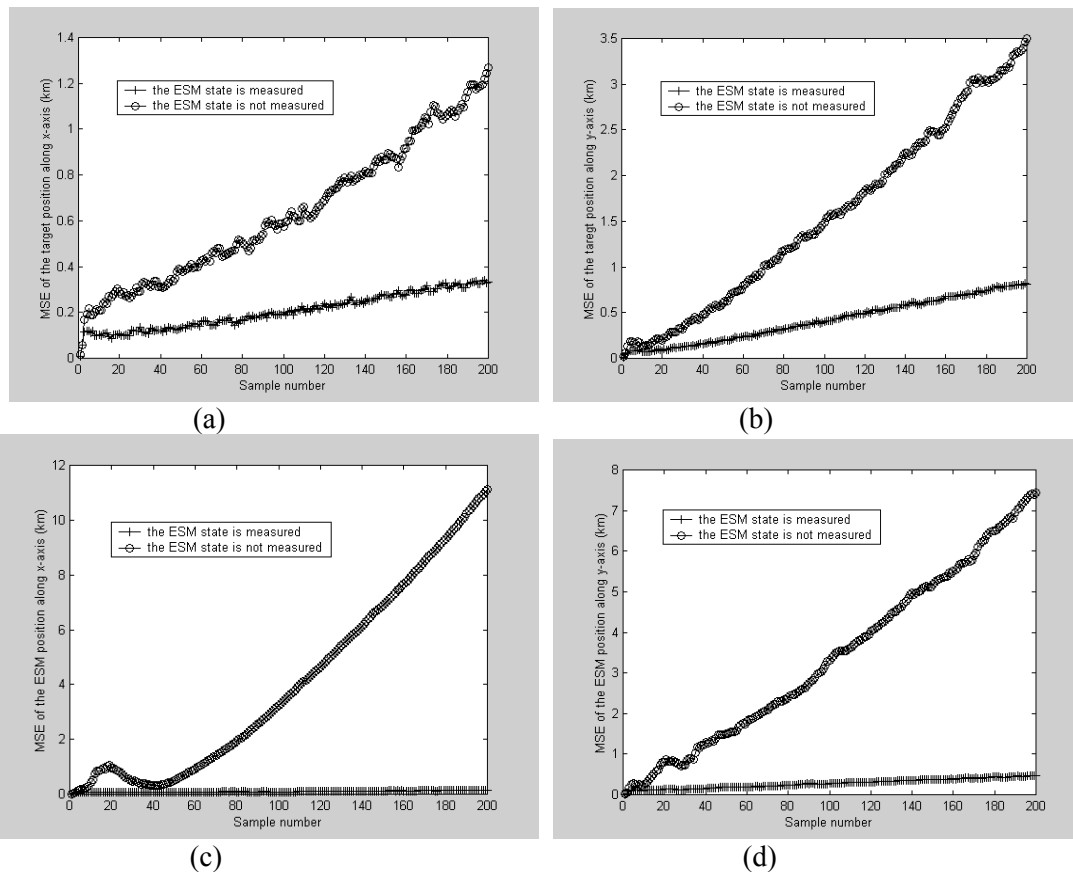


**Figure 7. Comparison of the state estimates with and without measuring the ESM sensor states: (a) the target position along x-axis; (b) the target position along y-axis; (c) the ESM position along x-axis; (d) the ESM position along y-axis.**

Figure 8 compares the sensitivity of the UKF and the EKF registration algorithms. The simulation results show that the EKF is very sensitive to the initial positions of the target and the ESM sensor, speeds along x- and y-axis, and sampling interval. For most track patterns, the EKF is divergent especially when the target and ESM sensor are close during some time intervals. This is due to the large biases that would be introduced in the estimates of the Jacobian matrix. Figure 8(a) shows one of the radar range estimates when the EKF is divergent. With selected parameters, the EKF can be made convergent. However, its accuracy is still low when compared with that of the UKF as shown in Figure 8(b). The reason is that the

absolute errors of the higher-order terms in estimating state mean and covariance are smaller for the unscented transformation in the UKF than for the linearization method in the EKF [22].

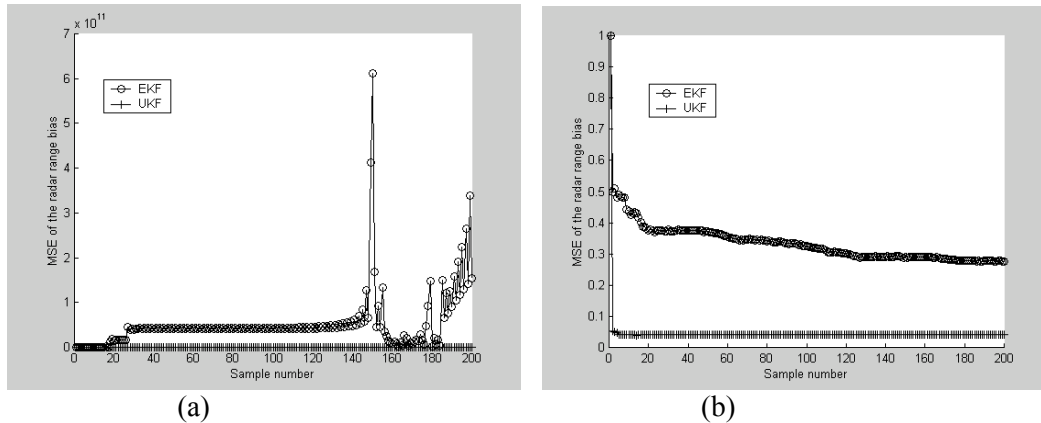


**Figure 8. Comparison of the EKF and UKF registration algorithms: (a) divergent EKF solution for radar range bias estimation; (b) convergent EKF for radar range bias estimation.**

## 4.2 Constant-acceleration targets

Now we consider the constant-acceleration targets. Two tracks and their radar measurements are shown in Figure 9(a). The fused tracks after registration are compared with the actual tracks in Figure 9(b). Figure 9 shows that the target state estimation by the UKF is closer to the actual tracks than the radar measurements. The detailed experimental results for one track in Figure 9 are presented below.

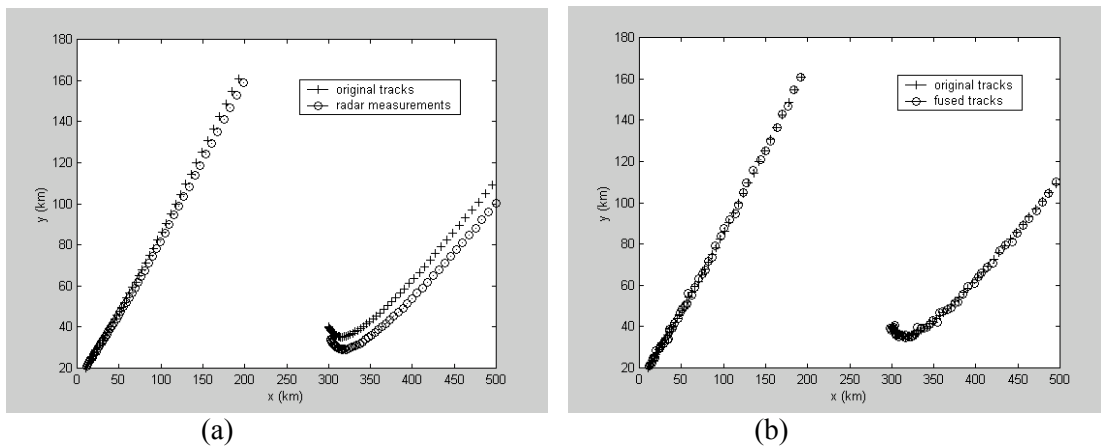


**Figure 9. Track plots of the constant-acceleration targets. (a) actual tracks and the radar measurements; (b) actual and fused tracks.**

Figures 10 and 11 show the MSEs of the system bias estimates of the radar and ESM sensor and the target state estimates, respectively, when the detection probability of the ESM sensor is set to 100%. The radar is located at (0, 0). The parameters of the target states are given by initial position: (10km, 20km), initial velocity: (0.40km/s, 0.60km/s), initial acceleration: (0.01 km/s<sup>2</sup>, 0.05 km/s<sup>2</sup>), standard deviation of dynamics:  $\delta_{\mu} = 0.04 \text{ km}$ . The parameters of the ESM sensor states are: initial position: (100km, 10km), initial velocity: (0.15km/s, 0.10km/s), initial acceleration: (0.02 km/s<sup>2</sup>, 0.04 km/s<sup>2</sup>), and standard deviation of dynamics:  $\delta_{\nu} = 0.02 \text{ km}$ . The measurement noise variances are 0.2 km and 0.002 rad for the radar and ESM sensor, respectively. The system biases are:  $\Delta t = 1.0 \text{ s}$ ,  $\Delta \theta_R = -0.01 \text{ rad}$ ,  $\Delta r_R = 1.0 \text{ km}$ ,  $\Delta \theta_E = 0.01 \text{ rad}$ . The radar measurement biases for the target states are shown in Figures 11(a) and 11(b) for comparison. We observe that the registration parameters and the target state estimates are close to the PCRBs for the constant-acceleration target. As shown in Figures 11(a) and 11(b), the estimation error of the target positions after registration is lower than the radar measurement biases.

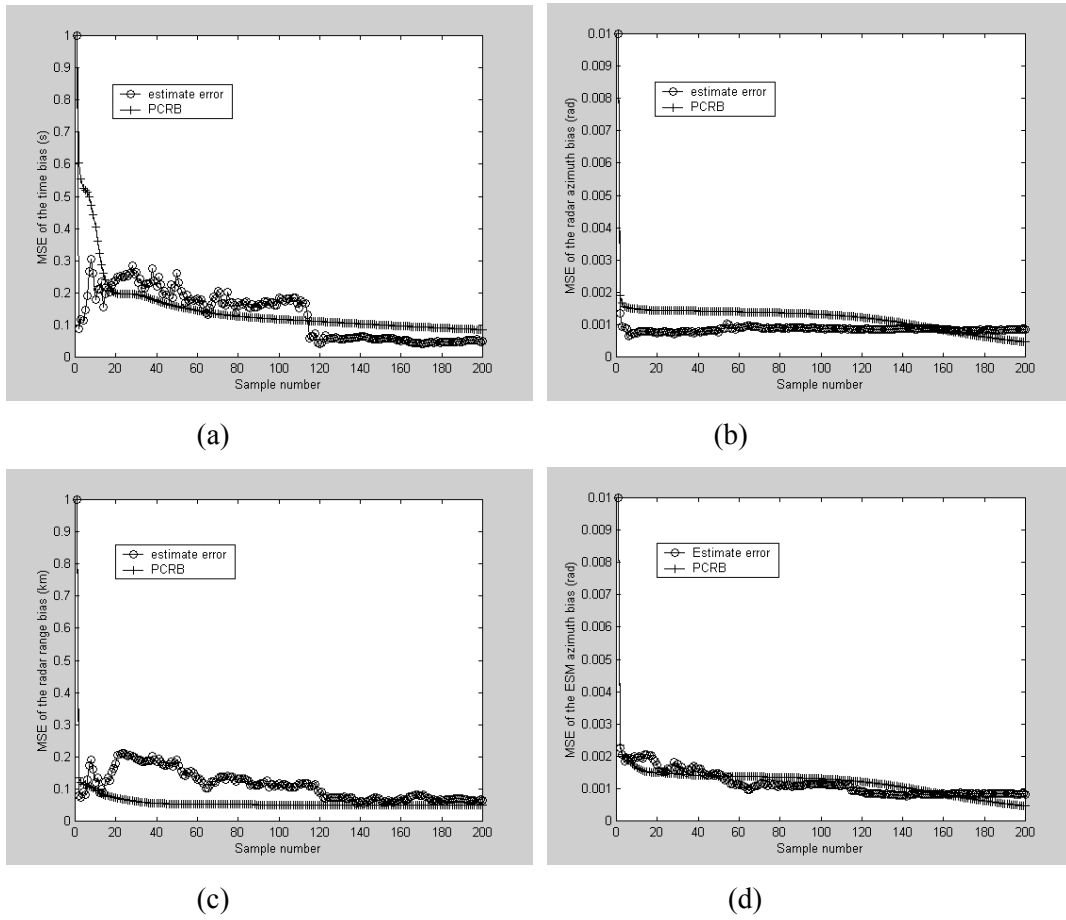
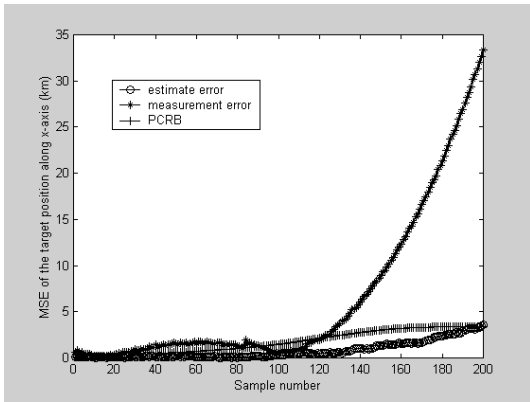
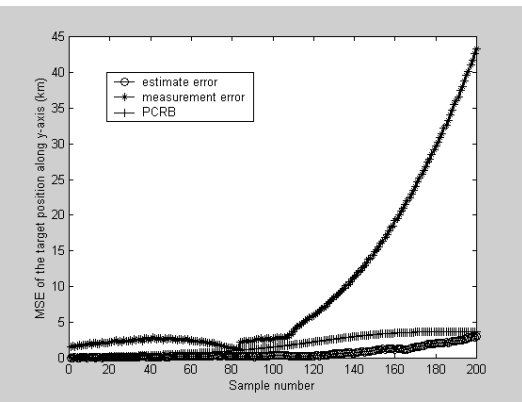


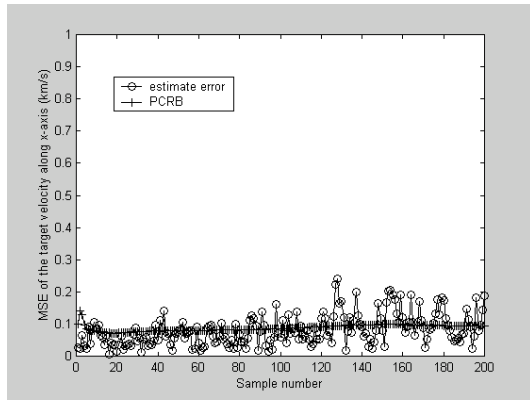
**Figure 10. Variation of the MSEs of the registration estimates versus the number of measurements for the constant-acceleration target and a unity detection probability for the ESM sensor: (a)  $\Delta t$ ; (b)  $\Delta\theta_R$ ; (c)  $\Delta r_R$ ; (d)  $\Delta\theta_E$ .**



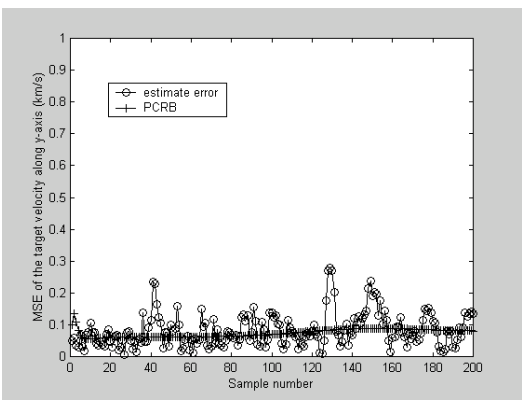
(a)



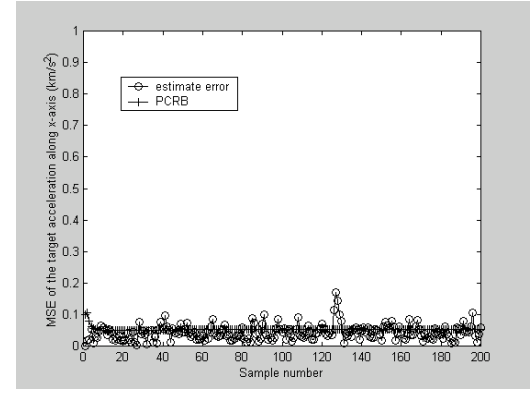
(b)



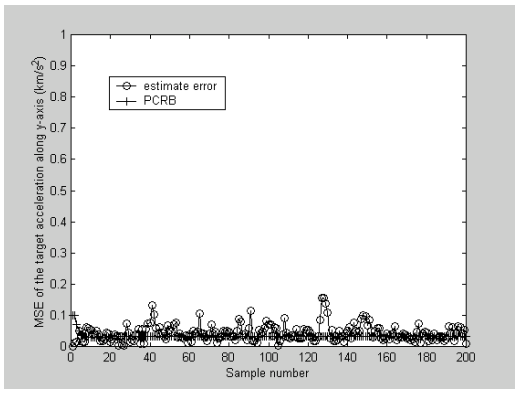
(c)



(d)



(e)



(f)

**Figure 11. Variation of the MSEs of the target state estimates versus the number of measurements for the constant-acceleration target and a unity detection probability for the ESM sensor: (a) position in x-axis; (b) position in y-axis; (c) velocity in x-axis; (d) velocity in y-axis; (e) acceleration in x-axis; (f) acceleration in y-axis.**



## 6. Conclusions

---

A novel registration algorithm has been proposed for mobile radar and ESM sensors with both space and time alignment errors. The algorithm is based on the application of the UKF, and uses an augmented state space model that includes the target state as well as the space and time alignment errors. The UKF is applied to estimate the sensor registration parameters and the target states simultaneously. The performance analysis of the algorithm was carried out. It was shown that the estimates of the target states by the UKF are unbiased if the space-time system biases are completely corrected. However, if the system biases are not completely corrected, then the target state estimates will be biased. Computer simulations were used to show the performance of the proposed UKF registration algorithm. Two types of targets were simulated: the constant velocity and the constant acceleration targets. Different detection probabilities were assumed for the ESM sensors. In each case, the Monte Carlo simulation results showed that the UKF estimates of the registration parameters and the target states have covariances that are close to the PCRBs under different track patterns and detection probabilities for the ESM sensor. Simulation studies also showed that the UKF is more stable than the EKF. The EKF is sensitive to the initial conditions of the target and the ESM sensor, and tended to diverge when the target and the ESM sensor were close during some time intervals. This is due to the large biases introduced in the estimates of the Jacobian matrix in the linearization process. In the simulation study, we manipulated the EKF to make it convergent. However, the UKF still showed superior performance in terms of estimation accuracy.

## 7. References

---

1. Brooks, R. R. (1998) *Multi-Sensor Fusion: Fundamentals and Applications with Software*, Upper Saddle River, NJ: Prentice Hall PTR, 1998
2. Blackman, S., and Popli, R. (1999) *Design and Analysis of Modern Tracking Systems*, Boston: Artech House, 1999
3. Saha, R. K. (1996) Track-to-track fusion with dissimilar sensors, *IEEE Trans. Aerospace and Electronic Systems*, 32, no. 3, pp.1021-1029
4. Wang, H., Mao, S. Y., He, Y., and Liu, Y. J. (2000) Triple-threshold radar-to-ESM correlation algorithm when each radar track is specified by different number of measurements, *IEE Proc. Radar. Sonar Navig.*, 147, no. 4, pp. 177-181
5. Challa, S., and Pulford, G. W. (2001) Joint target tracking and classification using radar and ESM sensors, *IEEE Trans. Aerospace and Electronics Systems*, 37, no. 3, pp. 1039-1055.
6. Kim, K. (1990) Integration of an electronic support measures (ESM) and an alpha-beta radar tracker, *Proc. SPIE*, vol. 1305, pp. 324-335
7. Watson, G. A., and Blair, W. D. (1990) Revisit control of a phased-array radar for tracking maneuvering targets when supported by a precise electronic support measures (ESM) sensor, *Proc. SPIE*, vol. 2235, pp. 448-459
8. Dana, M. P. (1990) Registration: a prerequisite for multiple sensor tracking. In *Multitarget-Multisensor Tracking: Advanced Applications*, Y. Barshalom, Ed., Norwood, MA: Artech House, 1990
9. Couture, J., Boily, E., and Simard, M. (1996) Sensor data fusion of radar, ESM, IFF, and data LINK of the Canadian patrol frigate and the data alignment issues, *Proc. SPIE*, vol. 2759, pp. 361-372
10. Kastella, K., Yearly, B., Zadra, T., Brouillard, R., and Frangione, E. (2000) Bias modeling and estimation for GMTI applications, In *Proc. 3<sup>rd</sup> International Conference on Information fusion*, Paris, France, July 2000
11. Fischer, W. L., Muehe, C. E., and Cameron, A. G. (1980) Registration errors in a netted surveillance system, *Report 1980-40*, MIT Lincoln Lab, Sept.1980
12. Zhou, Y., Leung, H., and Blanchette, M. (1999) Sensor alignment with earth-centered earth-fixed (ECEF) coordinate systems, *IEEE Trans. Aerospace and Electronic Systems*, 35, no. 2, pp. 410-417
13. Cowley, D. C., and Shafai, B. (1993) Registration in multi-sensor data fusion and tracking, In *Proc. of the American Control Conference*, San Francisco, CA, June 1993, pp. 875-879
14. Zhou, Y., Leung, H., and Yip, P. C. (1997) An exact maximum likelihood registration algorithm for data fusion, *IEEE Trans. Signal Processing*, 45, no. 6, pp. 1560-1572

15. McMichael, D. W., and Okello, N. N. (1996) Maximum likelihood registration of dissimilar sensors, In *Proc. Austr. Data Fusion Symp.*, Adelaide, Australia, 1996, pp. 31-34
16. Cruz, E. D., Alouani, A., Rice, T., and Blair, W. (1992) Sensor registration in multisensor systems, *Proc. SPIE*, vol. 1698, pp. 382-393
17. Zhou, Y., Leung, H., and Bosse, E. (1997) Registration of mobile sensors using the parallelized extended Kalman filter, *Opt. Eng.*, 36, no. 3, pp. 780-788
18. Chansarkar, M., and Kohli, S. (1999) Solution to a multisensor tracking problem with sensor registration errors, *IEEE Trans. Aerospace and Electronic Systems*, 35, no. 1, pp. 354-363
19. Okello, N. N., and Pulford, G. W. (1996) Simultaneous registration and tracking for multiple radars with cluttered measurements, In *Proc. of 8<sup>th</sup> IEEE Signal Processing Workshop on Statistical Signal and Array Processing*, Corfu, Greece, June 1996, pp. 60-63
20. Bar-Shalom, Y. (2000) Mobile radar bias estimation using unknown location targets, In *Proc. 3<sup>rd</sup> International Conference on Information fusion*, Paris, France, July 2000
21. Julier, S., Uhlmann, J., and Durrant-Whyte, H. F. (2000) A new method for the nonlinear transformation of means and covariances in filters and estimators. *IEEE Trans. Automatic Control*, 45, no. 3, pp. 477-482
22. Wan, E. A., and van der Merwe, R. (2001) The unscented Kalman filter □ In *Kalman Filter and Neural Networks*, S. Haykin, Ed., Wiley Publishing, 2001
23. Wan, E. A., and van der Merwe, R. (2000) The unscented Kalman filter for nonlinear estimation, In *IEEE Proceedings of Symposium on Adaptive Systems for Signal Processing, Communication and Control*, Lake Louise, Alberta, Canada, Oct. 2000
24. Taylor, J. H. (1979) The Cramer-Rao estimation error lower bound computation for deterministic nonlinear systems, *IEEE Trans. Automatic Control*, 24, no. 2, pp. 343-344
25. Zhou, Y., Yip, P. C., and Leung, H. (1999) Tracking the direction-of-arrival of multiple moving targets by passive arrays: asymptotic performance analysis, *IEEE Trans. Signal Processing*, 47, no. 10, pp. 2644-2654
26. Tichavsky, P., Muravchik, C. H., and Nehorai, A. (1998) Posterior Cramer-Rao bounds for discrete-time nonlinear filtering, *IEEE Trans. Signal Processing*, 46, no. 5, pp. 1386-1396
27. Farina, A., Ristic, B., and Timmoneri, L. (2002) Cramer-Rao bound for nonlinear filtering with  $P_d < 1$  and its application to target tracking, *IEEE Trans. Signal Processing*, 50, no. 8, pp. 1916-1924
28. Caffery, J., Jr. and Stuber, G. L. (2000) Nonlinear multiuser parameter estimation and tracking in CDMA systems, *IEEE Trans. Communications*, 48, no. 12, pp. 2053-2063
29. Anderson, T. W. (1984) *An Introduction to Multivariate Statistical Analysis*. New York: Wiley

30. Gelb, A. (1988) *Applied Optimization Estimation*. Cambridge: MIT Press

## Annex A

---

The EKF algorithm for the augmented system (16) and (17) is given as follows. An EKF algorithm consists of two sets of equations: time update and measurement update equations. The time update equations predict the state and error covariance by using the current state estimate. The measurement update equations obtain a posterior estimate of the state by a new measurement and the prior state estimate.

*Time update equations:* The one-step prediction of  $\hat{\mathbf{X}}(t_{k-1})$  is

$$\hat{\mathbf{X}}^-(t_k) = \mathbf{F}\hat{\mathbf{X}}(t_{k-1}), \quad (67)$$

and the covariance matrix of the prediction error is

$$\mathbf{P}^-(t_k) = \mathbf{F}\mathbf{P}(t_{k-1})\mathbf{F}^T + \mathbf{R}_X. \quad (68)$$

*Measurement update equations:* The filtered estimate of the state  $\mathbf{X}(t_k)$  is given by

$$\hat{\mathbf{X}}(t_k) = \hat{\mathbf{X}}^-(t_k) + \mathbf{G}(t_k)[\mathbf{Z}(t_k) - \mathbf{h}(\hat{\mathbf{X}}^-(t_k))], \quad (69)$$

where the Kalman filter gain is determined by

$$\mathbf{G}(t_k) = \mathbf{P}^-(t_k)\mathbf{H}(t_k)[\mathbf{H}(t_k)\mathbf{P}^-(t_k)\mathbf{H}^T(t_k) + \mathbf{R}_z]^{-1}, \quad (70)$$

and  $\mathbf{H}(t_k) = (\partial\mathbf{h}(\mathbf{X})/\partial\mathbf{X})|_{\mathbf{X}=\hat{\mathbf{X}}(t_k)}$ . The covariance of the estimation error in  $\hat{\mathbf{X}}(t_k)$  is updated by

$$\mathbf{P}(t_k) = [\mathbf{I} - \mathbf{G}(t_k)\mathbf{H}(t_k)]\mathbf{P}^-(t_k). \quad (71)$$

## Annex B

$\mathbf{H}_1(t_k)$  and  $\mathbf{H}_2(t_k)$  are defined by

$$\begin{aligned}\mathbf{H}_1(t_k) &= \frac{\partial(\mathbf{h}(\mathbf{X}^{(1)}(t_k), \mathbf{X}^{(2)}(t_k), \mathbf{X}^{(1)}(t_{k+1}), \mathbf{S}_l(t_{k+1})))}{\partial \mathbf{X}^{(1)}(t_{k+1})} \\ &= \left[ \frac{\partial h_1^T(t_{k+1})}{\partial \mathbf{X}^{(1)}(t_{k+1})}, \frac{\partial h_2^T(t_{k+1})}{\partial \mathbf{X}^{(1)}(t_{k+1})}, \frac{\partial h_3^T(t_{k+1})}{\partial \mathbf{X}^{(1)}(t_{k+1})}, \frac{\partial h_4^T(t_{k+1})}{\partial \mathbf{X}^{(1)}(t_{k+1})}, \frac{\partial h_5^T(t_{k+1})}{\partial \mathbf{X}^{(1)}(t_{k+1})} \right]^T,\end{aligned}$$

and

$$\begin{aligned}\mathbf{H}_2(t_k) &= \frac{\partial(\mathbf{h}(\mathbf{X}^{(1)}(t_k), \mathbf{X}^{(2)}(t_k), \mathbf{X}^{(1)}(t_{k+1}), \mathbf{S}_l(t_{k+1})))}{\partial \mathbf{X}^{(2)}(t_k)} \\ &= \left[ \frac{\partial h_1^T(t_{k+1})}{\partial \mathbf{X}^{(2)}(t_k)}, \frac{\partial h_2^T(t_{k+1})}{\partial \mathbf{X}^{(2)}(t_k)}, \frac{\partial h_3^T(t_{k+1})}{\partial \mathbf{X}^{(1)}(t_k)}, \frac{\partial h_4^T(t_{k+1})}{\partial \mathbf{X}^{(2)}(t_k)}, \frac{\partial h_5^T(t_{k+1})}{\partial \mathbf{X}^{(1)}(t_k)} \right]^T.\end{aligned}$$

$\mathbf{X}^{(2)}(t_k) = [\Delta t, \Delta \theta_R, \Delta r_R, \Delta \theta_E]^T$  represents the biases of the sensors while  $\mathbf{X}^{(1)}(t_k)$  is the states of the target and ESM, and

$$\mathbf{X}^{(1)}(t_k) = [x_R(t_k), \dot{x}_R(t_k), y_R(t_k), \dot{y}_R(t_k), u(t_k), \dot{u}(t_k), v(t_k), \dot{v}(t_k)]^T,$$

for the constant-velocity state model. Using the definitions of  $\mathbf{h}(t_k)$  in (18) and (19), we can derive the elements of the Jacobian matrix.  $\mathbf{H}_1(t_k)$  can be expressed by

$$\begin{aligned}\frac{\partial h_1(t_{k+1})}{\partial x_R(t_{k+1})} &= 1 + \frac{y_R^2(t_{k+1})}{[x_R^2(t_{k+1}) + y_R^2(t_{k+1})]^{3/2}} \Delta r_R, \quad \frac{\partial h_1(t_{k+1})}{\partial \dot{x}_R(t_{k+1})} = \Delta t, \\ \frac{\partial h_1(t_{k+1})}{\partial y_R(t_{k+1})} &= \Delta \theta_R - \frac{x_R(t_{k+1})y_R(t_{k+1})}{[x_R^2(t_{k+1}) + y_R^2(t_{k+1})]^{3/2}} \Delta r_R, \quad \frac{\partial h_1(t_{k+1})}{\partial \dot{y}_R(t_{k+1})} = 0, \\ \frac{\partial h_1(t_{k+1})}{\partial u(t_{k+1})} &= \frac{\partial h_1(t_{k+1})}{\partial \dot{u}(t_{k+1})} = \frac{\partial h_1(t_{k+1})}{\partial v(t_{k+1})} = \frac{\partial h_1(t_{k+1})}{\partial \dot{v}(t_{k+1})} = 0, \\ \frac{\partial h_2(t_{k+1})}{\partial x_R(t_{k+1})} &= -\Delta \theta_R - \frac{x_R(t_{k+1})y_R(t_{k+1})}{[x_R^2(t_{k+1}) + y_R^2(t_{k+1})]^{3/2}} \Delta r_R, \quad \frac{\partial h_2(t_{k+1})}{\partial \dot{x}_R(t_{k+1})} = 0, \\ \frac{\partial h_2(t_{k+1})}{\partial y_R(t_{k+1})} &= 1 + \frac{x_R^2(t_{k+1})}{[x_R^2(t_{k+1}) + y_R^2(t_{k+1})]^{3/2}} \Delta r_R, \quad \frac{\partial h_2(t_{k+1})}{\partial \dot{y}_R(t_{k+1})} = \Delta t, \\ \frac{\partial h_2(t_{k+1})}{\partial u(t_{k+1})} &= \frac{\partial h_2(t_{k+1})}{\partial \dot{u}(t_{k+1})} = \frac{\partial h_2(t_{k+1})}{\partial v(t_{k+1})} = \frac{\partial h_2(t_{k+1})}{\partial \dot{v}(t_{k+1})} = 0,\end{aligned}$$

$$\begin{aligned}
\frac{\partial h_3(t_{k+1})}{\partial x_R(t_{k+1})} &= s_l(t_{k+1}) \frac{[y_R(t_{k+1}) - v(t_{k+1})]}{[x_R(t_{k+1}) - u(t_{k+1})]^2 + [y_R(t_{k+1}) - v(t_{k+1})]^2}, \quad \frac{\partial h_3(t_{k+1})}{\partial \dot{x}_R(t_{k+1})} = 0, \\
\frac{\partial h_3(t_{k+1})}{\partial y_R(t_{k+1})} &= -s_l(t_{k+1}) \frac{[x_R(t_{k+1}) - u(t_{k+1})]}{[x_R(t_{k+1}) - u(t_{k+1})]^2 + [y_R(t_{k+1}) - v(t_{k+1})]^2}, \quad \frac{\partial h_3(t_{k+1})}{\partial \dot{y}_R(t_{k+1})} = 0, \\
\frac{\partial h_3(t_{k+1})}{\partial u(t_{k+1})} &= s_l(t_{k+1}) \frac{[y_R(t_{k+1}) - v(t_{k+1})]}{[x_R(t_{k+1}) - u(t_{k+1})]^2 + [y_R(t_{k+1}) - v(t_{k+1})]^2}, \quad \frac{\partial h_3(t_{k+1})}{\partial \dot{u}(t_{k+1})} = 0, \\
\frac{\partial h_3(t_{k+1})}{\partial v(t_{k+1})} &= s_l(t_{k+1}) \frac{[x_R(t_{k+1}) - u(t_{k+1})]}{[x_R(t_{k+1}) - u(t_{k+1})]^2 + [y_R(t_{k+1}) - v(t_{k+1})]^2}, \quad \frac{\partial h_3(t_{k+1})}{\partial \dot{v}(t_{k+1})} = 0, \\
\frac{\partial h_4(t_{k+1})}{\partial x_R(t_{k+1})} &= \frac{\partial h_4(t_{k+1})}{\partial \dot{x}_R(t_{k+1})} = \frac{\partial h_4(t_{k+1})}{\partial y_R(t_{k+1})} = \frac{\partial h_4(t_{k+1})}{\partial \dot{y}_R(t_{k+1})} = 0, \\
\frac{\partial h_4(t_{k+1})}{\partial u(t_{k+1})} &= 1 + \frac{v^2(t_{k+1})}{[u^2(t_{k+1}) + v^2(t_{k+1})]^{3/2}} \Delta r_R, \quad \frac{\partial h_4(t_{k+1})}{\partial \dot{u}(t_{k+1})} = \Delta t, \\
\frac{\partial h_4(t_{k+1})}{\partial v(t_{k+1})} &= \Delta \theta_R - \frac{u(t_{k+1})v(t_{k+1})}{[u^2(t_{k+1}) + v^2(t_{k+1})]^{3/2}} \Delta r_R, \quad \frac{\partial h_4(t_{k+1})}{\partial \dot{v}(t_{k+1})} = 0, \\
\frac{\partial h_5(t_{k+1})}{\partial x_R(t_{k+1})} &= \frac{\partial h_5(t_{k+1})}{\partial \dot{x}_R(t_{k+1})} = \frac{\partial h_5(t_{k+1})}{\partial y_R(t_{k+1})} = \frac{\partial h_5(t_{k+1})}{\partial \dot{y}_R(t_{k+1})} = 0, \\
\frac{\partial h_5(t_{k+1})}{\partial u(t_{k+1})} &= -\Delta \theta_R - \frac{u(t_{k+1})v(t_{k+1})}{[u^2(t_{k+1}) + v^2(t_{k+1})]^{3/2}} \Delta r_R, \quad \frac{\partial h_5(t_{k+1})}{\partial \dot{u}(t_{k+1})} = 0, \\
\frac{\partial h_5(t_{k+1})}{\partial v(t_{k+1})} &= 1 + \frac{u^2(t_{k+1})}{[u^2(t_{k+1}) + v^2(t_{k+1})]^{3/2}} \Delta r_R, \quad \frac{\partial h_5(t_{k+1})}{\partial \dot{v}(t_{k+1})} = \Delta t. \tag{72}
\end{aligned}$$

$H_2(t_k)$  is given by

$$\begin{aligned}
\frac{\partial h_1(t_{k+1})}{\partial \Delta t} &= \dot{x}_R(t_{k+1}), \quad \frac{\partial h_1(t_{k+1})}{\partial \Delta \theta_R} = y_R(t_{k+1}), \quad \frac{\partial h_1(t_{k+1})}{\partial \Delta r_R} = \frac{x_R(t_{k+1})}{[x_R^2(t_{k+1}) + y_R^2(t_{k+1})]^{1/2}}, \\
\frac{\partial h_1(t_{k+1})}{\partial \theta_E} &= 0, \quad \frac{\partial h_2(t_{k+1})}{\partial \Delta t} = \dot{y}_R(t_{k+1}), \quad \frac{\partial h_2(t_{k+1})}{\partial \Delta \theta_R} = -x_R(t_{k+1}), \\
\frac{\partial h_2(t_{k+1})}{\partial \Delta r_R} &= \frac{y_R(t_{k+1})}{[x_R^2(t_{k+1}) + y_R^2(t_{k+1})]^{1/2}}, \quad \frac{\partial h_1(t_{k+1})}{\partial \theta_E} = 0, \quad \frac{\partial h_3(t_{k+1})}{\partial \Delta t} = 0, \\
\frac{\partial h_3(t_{k+1})}{\partial \Delta \theta_R} &= 0, \quad \frac{\partial h_3(t_{k+1})}{\partial \Delta r_R} = 0, \quad \frac{\partial h_3(t_{k+1})}{\partial \Delta \theta_E} = s_l(t_{k+1}),
\end{aligned}$$

$$\begin{aligned}
\frac{\partial h_4(t_{k+1})}{\partial \Delta t} &= \dot{u}(t_{k+1}), \quad \frac{\partial h_4(t_{k+1})}{\partial \Delta \theta_R} = v(t_{k+1}), \quad \frac{\partial h_4(t_{k+1})}{\partial \Delta r_R} = \frac{u(t_{k+1})}{[u^2(t_{k+1}) + v^2(t_{k+1})]^{1/2}}, \\
\frac{\partial h_4(t_{k+1})}{\partial \Delta \theta_E} &= 0, \quad \frac{\partial h_5(t_{k+1})}{\partial \Delta t} = \dot{v}(t_{k+1}), \quad \frac{\partial h_5(t_{k+1})}{\partial \Delta \theta_R} = -u(t_{k+1}), \\
\frac{\partial h_5(t_{k+1})}{\partial \Delta r_R} &= \frac{v(t_{k+1})}{[u^2(t_{k+1}) + v^2(t_{k+1})]^{1/2}}, \quad \frac{\partial h_5(t_{k+1})}{\partial \Delta \theta_E} = 0.
\end{aligned} \tag{73}$$



**UNCLASSIFIED**

SECURITY CLASSIFICATION OF FORM  
(highest classification of Title, Abstract, Keywords)

**DOCUMENT CONTROL DATA**

(Security classification of title, body of abstract and indexing annotation must be entered when the overall document is classified)

1. ORIGINATOR (the name and address of the organization preparing the document. Organizations for whom the document was prepared, e.g. Establishment sponsoring a contractor's report, or tasking agency, are entered in section 8.)  Defence R&D Canada – Ottawa		2. SECURITY CLASSIFICATION (overall security classification of the document, including special warning terms if applicable)  UNCLASSIFIED	
3. TITLE (the complete document title as indicated on the title page. Its classification should be indicated by the appropriate abbreviation (S,C or U) in parentheses after the title.)  Unscented Kalman Filter Based Spatial-Temporal Registration Approach for Mobile Radar and ESM Sensors			
4. AUTHORS (Last name, first name, middle initial)  Yifeng Zhou, Winston Li and Henry Leung			
5. DATE OF PUBLICATION (month and year of publication of document)  December 2003		6a. NO. OF PAGES (total containing information. Include Annexes, Appendices, etc.)  47	6b. NO. OF REFS (total cited in document)  30
7. DESCRIPTIVE NOTES (the category of the document, e.g. technical report, technical note or memorandum. If appropriate, enter the type of report, e.g. interim, progress, summary, annual or final. Give the inclusive dates when a specific reporting period is covered.)  DRDC Ottawa Technical Report			
8. SPONSORING ACTIVITY (the name of the department project office or laboratory sponsoring the research and development. Include the address.)  DRDC Ottawa			
9a. PROJECT OR GRANT NO. (if appropriate, the applicable research and development project or grant number under which the document was written. Please specify whether project or grant)  1ac11 & 15bb29		9b. CONTRACT NO. (if appropriate, the applicable number under which the document was written)	
10a. ORIGINATOR'S DOCUMENT NUMBER (the official document number by which the document is identified by the originating activity. This number must be unique to this document.)  DRDC Ottawa TR 2003-219		10b. OTHER DOCUMENT NOS. (Any other numbers which may be assigned this document either by the originator or by the sponsor)	
11. DOCUMENT AVAILABILITY (any limitations on further dissemination of the document, other than those imposed by security classification)  <input checked="" type="checkbox"/> Unlimited distribution <input type="checkbox"/> Distribution limited to defence departments and defence contractors; further distribution only as approved <input type="checkbox"/> Distribution limited to defence departments and Canadian defence contractors; further distribution only as approved <input type="checkbox"/> Distribution limited to government departments and agencies; further distribution only as approved <input type="checkbox"/> Distribution limited to defence departments; further distribution only as approved <input type="checkbox"/> Other (please specify):			
12. DOCUMENT ANNOUNCEMENT (any limitation to the bibliographic announcement of this document. This will normally correspond to the Document Availability (11). However, where further distribution (beyond the audience specified in 11) is possible, a wider announcement audience may be selected.)  Full Unlimited Announcement			

**UNCLASSIFIED**

SECURITY CLASSIFICATION OF FORM

13. ABSTRACT (a brief and factual summary of the document. It may also appear elsewhere in the body of the document itself. It is highly desirable that the abstract of classified documents be unclassified. Each paragraph of the abstract shall begin with an indication of the security classification of the information in the paragraph (unless the document itself is unclassified) represented as (S), (C), or (U). It is not necessary to include here abstracts in both official languages unless the text is bilingual).

Space and time alignments are prerequisites for the successful fusion of multiple sensors. In this report, a space-time registration model is proposed for estimating the system biases and performing time synchronization for mobile radar and electronic support measure (ESM) systems. A space-time registration model for radar and ESM sensors is first developed, and an unscented Kalman filter (UKF) is proposed to estimate the space-time biases and target states simultaneously. The posterior Cramer-Rao bounds (PCRBs) are derived for the proposed UKF registration algorithm for ESM detection probability less than or equal to one. Theoretical analysis is performed for evaluating the accuracy and robustness of the proposed algorithm. Computer simulations are used to demonstrate the effectiveness and robustness of the proposed algorithm under different radar and ESM tracking scenarios.

14. KEYWORDS, DESCRIPTORS or IDENTIFIERS (technically meaningful terms or short phrases that characterize a document and could be helpful in cataloguing the document. They should be selected so that no security classification is required. Identifiers such as equipment model designation, trade name, military project code name, geographic location may also be included. If possible keywords should be selected from a published thesaurus. e.g. Thesaurus of Engineering and Scientific Terms (TEST) and that thesaurus-identified. If it is not possible to select indexing terms which are Unclassified, the classification of each should be indicated as with the title.)

ESM sensor, radar, registration, Kalman, unscented, detection and estimation, fusion, mobile sensor, tracking



## **Defence R&D Canada**

Canada's leader in defence  
and national security R&D

## **R & D pour la défense Canada**

Chef de file au Canada en R & D  
pour la défense et la sécurité nationale



[www.drdc-rddc.gc.ca](http://www.drdc-rddc.gc.ca)